

2010

# Synthesis of aza-bridged tetraphosphine ligands for a dirhodium hydroformylation catalyst

Scott Michael Boudreaux

*Louisiana State University and Agricultural and Mechanical College*

Follow this and additional works at: [https://digitalcommons.lsu.edu/gradschool\\_theses](https://digitalcommons.lsu.edu/gradschool_theses)

 Part of the [Chemistry Commons](#)

---

## Recommended Citation

Boudreaux, Scott Michael, "Synthesis of aza-bridged tetraphosphine ligands for a dirhodium hydroformylation catalyst" (2010). *LSU Master's Theses*. 104.

[https://digitalcommons.lsu.edu/gradschool\\_theses/104](https://digitalcommons.lsu.edu/gradschool_theses/104)

This Thesis is brought to you for free and open access by the Graduate School at LSU Digital Commons. It has been accepted for inclusion in LSU Master's Theses by an authorized graduate school editor of LSU Digital Commons. For more information, please contact [gradetd@lsu.edu](mailto:gradetd@lsu.edu).

SYNTHESIS OF AZA-BRIDGED TETRAPHOSPHINE LIGANDS FOR A DIRHODIUM  
HYDROFORMYLATION CATALYST

A Thesis

Submitted to the Graduate Faculty of the  
Louisiana State University and  
Agricultural and Mechanical College  
In partial fulfillment of the  
Requirements for the degree of  
Master of Science

in

The Department of Chemistry

by  
Scott M. Boudreaux  
B.S. Nicholls State University, 2007  
May, 2010

## TABLE OF CONTENTS

LIST OF TABLES.....	iv
LIST OF FIGURES .....	v
ABSTRACT.....	viii
CHAPTER 1: HYDROFORMYLATION .....	1
1.1. Introduction to Hydroformylation .....	1
1.2. Cobalt Hydroformylation Catalysts .....	1
1.3. Rhodium Hydroformylation Catalysts .....	3
1.4. Mono- and Bis- Phosphines and Phosphite Ligands For Hydroformylation Catalysts .....	5
1.5. References.....	9
CHAPTER 2: BIMETALLIC COOPERATIVITY IN HYDROFORMYLATION .....	11
2.1. Introduction .....	11
2.2. Discovery of a Cooperative Dirhodium Catalyst .....	12
2.3. Confirmation of Bimetallic Cooperativity .....	14
2.4. Polar-Phase Hydroformylation .....	15
2.5. H <sub>2</sub> /CO Ratio Studies .....	16
2.6. References .....	18
CHAPTER 3: DESIGN AND SYNTHESIS OF AZA-BRIDGED TETRAPHOSPHINE LIGANDS .....	19
3.1. Introduction .....	19
3.2. Evolution of the P <sub>4</sub> Ligand .....	21
3.3. Changes in the Catalyst by Ligand Variation .....	23
3.3.1 The et,ph-P <sub>4</sub> Ligand.....	23
3.3.2 The et,ph-P <sub>4</sub> -Ph (aka P <sub>4</sub> -Ph) Ligand.....	24
3.3.3 The RN-P <sub>4</sub> -Ph Ligands .....	24
3.4. Fragmentation and Side Reactions of PNP Ligands.....	26
3.5. Applications .....	28
3.6. Retrosynthetic Analysis of the Aza-Bridged Ligand .....	30
3.7. Synthesis of RN-P <sub>4</sub> -Ph by "Large Arm"-Amine Coupling .....	30
3.8. Synthesis of Rn-P <sub>4</sub> -Ph by Grignard-mediated "Small Arm"-Amine Bridge Coupling .....	34
3.9. Future Work .....	38
3.10. References .....	39
CHAPTER 4: EXPERIMENTAL SECTION.....	40
4.1. Synthesis of (2-bromophenyl)diethylphosphine .....	40
4.2. Synthesis of Chloro(N,N-diethylamino)phenylphosphine .....	41
4.3. Attempted Synthesis of (N,N-diethylamino)(2-(diethylphosphino)phenyl)- phenylphosphine .....	42
4.4. Attempted Synthesis of Chloro(2-(diethylphosphino)phenyl)phenylphosphine ...	43
4.5. Attempted Synthesis of Bis(chlorophenylphosphino)cyclohexylamine .....	44
4.6. Attempted Synthesis of Bis(chlorophenylphosphino)ethylamine.....	45

4.7. Attempted Synthesis of Bis(chlorophenylphosphino) <sup>t</sup> butylamine .....	45
4.8. Attempted Synthesis of Bis(chlorophenylphosphino) <i>p</i> - <sup>t</sup> butylaniline .....	46
4.9. Synthesis of Phenylphosphine .....	47
4.10. Synthesis of Bis(phenylphosphino)methane.....	48
4.11. Synthesis of Diethylchlorophosphine.....	49
4.12. Synthesis of Vinyl-diethylphosphine .....	49
4.13. Synthesis of <i>racemic</i> and <i>meso</i> et,ph-P4 .....	50
VITA.....	52

## LIST OF TABLES

2.1. Hydroformylation* of 1-hexene .....	15
2.2. Rh <sub>2</sub> hydroformylation data from variable H <sub>2</sub> /CO ratio and pressure studies. ....	17

## LIST OF FIGURES

1.1. General hydroformylation reaction scheme. ....	1
1.2. Commercially employed reactions of aldehydes. ....	2
1.3. Heck-Breslow cobalt-catalyzed hydroformylation mechanism. ....	3
1.4. Proposed mechanism for rhodium-catalyzed hydroformylation. ....	4
1.5. Various ligands used in biphasic hydroformylation. ....	6
1.6. Bulky bisphosphite ligands. ....	8
1.7. BISBI; Introduced to hydroformylation by Tom Devon. ....	8
1.8. Examples from the Xantphos series and their calculated natural bite angles. ....	9
2.1. Proposed bimetallic pathway by Heck. ....	11
2.2. Synthesis of <i>meso</i> and <i>racemic</i> et,ph-P4. ....	12
2.3. Synthesis of the catalyst precursor, <i>rac</i> -[Rh <sub>2</sub> H <sub>2</sub> (□-CO) <sub>2</sub> (et,ph-P4)] <sup>2+</sup> ....	12
2.4. Open- and closed-mode dirhodium complexes. ....	13
2.5. Intramolecular hydride transfer in <i>racemic</i> and <i>meso</i> catalysts. ....	13
2.6. Stanley's proposed bimetallic hydroformylation mechanism. ....	14
2.7. Spaced bimetallic analogs. ....	15
3.1. Routes to ligand decomposition. ....	20
3.2. Proposed fragmentation pathway for the dirhodium catalyst. ....	21
3.3. Synthetic scheme for the et,ph-P4-Ph ligand. ....	22
3.4. Et,ph-P4-Ph with para-substituted internal phenyl rings. ....	22
3.5. The new aza-bridged et,ph-P4-Ph ligand. ....	23
3.6. Some examples of PNP-metal complexes. ....	26
3.7. Some examples of metal assisted cleavage of PNP ligands. ....	26
3.8. Fragmentation of PNP ligands via reaction with aldehydes ....	27
3.9. Proposed mechanism for C-insertion into a P-N bond. ....	27
3.10. Pudovik and Abramov reactions. ....	28

3.11. Bimetallic cobalt catalyst for asymmetric Pauson-Khand reactions.....	29
3.12. Isoprene trimerisation catalyst and ethylene polymerization catalyst. ....	29
3.13. Retrosynthetic analysis of RN-P4-Ph ligands. ....	30
3.14. Preparation of (a) ((2-bromophenyl)diethylphosphine) and (b) chloro(2-(diethylphosphino)phenyl)phenylphosphine utilizing halide-magnesium exchange reactions .....	31
3.15. $^{31}\text{P}\{^1\text{H}\}$ NMR of heptane and benzene extraction of the large arm.....	31
3.16. $^{31}\text{P}\{^1\text{H}\}$ NMR of (N,N-diethylamino)[2(diethylphosphino)phenyl]phenylphosphine..	32
3.17. $^{31}\text{P}\{^1\text{H}\}$ NMR spectra of products obtained from the deprotection of the mono-protected large arm. ....	33
3.18. $^{31}\text{P}\{^1\text{H}\}$ NMR of what might be (N,N-diethylamino)[2(diethylphosphino)- phenyl]phenylphosphine from most recent synthesis.....	34
3.19. Synthetic scheme involving a Grignard-mediated coupling.....	35
3.20. $^{31}\text{P}\{^1\text{H}\}$ NMR of t-butyl amine bridge after the initial reaction and second amine addition.....	35
3.21. $^{31}\text{P}\{^1\text{H}\}$ NMR of the initial reaction to form p-tert-butyl aniline bridge and after distillation.....	36
3.22. Synthesis of RN-P4-Ph utilizing the Finkelstein reaction.. ....	38
4.1. $^{31}\text{P}\{^1\text{H}\}$ NMR of (2-bromophenyl)diethylphosphine .....	42
4.2. $^{31}\text{P}\{^1\text{H}\}$ NMR of chloro(N,N-diethylamino)phenylphosphine .....	43
4.3. $^{31}\text{P}\{^1\text{H}\}$ NMR of (N,N-diethylamino)(2-(diethylphosphine)phenyl) phosphine.....	44
4.4. $^{31}\text{P}\{^1\text{H}\}$ NMR of the products obtained in the synthesis of chloro(2-(diethylphosphino)phenyl)phenylphosphine .....	45
4.5. $^{31}\text{P}\{^1\text{H}\}$ NMR of bis(chlorophenylphosphino)cyclohexylamine.....	46
4.6. $^{31}\text{P}\{^1\text{H}\}$ NMR of bis(chlorophenylphosphino)ethylamine.....	47
4.7. $^{31}\text{P}\{^1\text{H}\}$ NMR of bis(chlorophenylphosphino) <sup>t</sup> butylamine .....	48
4.8. $^{31}\text{P}\{^1\text{H}\}$ NMR of bis(chlorophenylphosphino) <i>p</i> - <sup>t</sup> butylaniline .....	49
4.9. $^{31}\text{P}\{^1\text{H}\}$ NMR of phenylphosphine .....	49

4.10. $^{31}\text{P}\{^1\text{H}\}$ NMR of bis(phenylphosphino)methane .....	50
4.11. $^{31}\text{P}\{^1\text{H}\}$ NMR of diethylchlorophosphine.....	51
4.12. $^{31}\text{P}\{^1\text{H}\}$ NMR of vinyl-diethylphosphine .....	52
4.13. $^{31}\text{P}\{^1\text{H}\}$ NMR of <i>racemic</i> and <i>meso</i> et,ph-P4.....	52



## ABSTRACT

A novel tetraphosphine ligand *rac*-*et,ph*-P4 (*et,ph*-P4 =  $\text{PEt}_2\text{CH}_2\text{CH}_2(\text{Ph})\text{PCH}_2\text{P}(\text{Ph})\text{CH}_2\text{CH}_2\text{PEt}_2$ ) is used for the formation of a highly active and regioselective hydroformylation catalyst. The active catalytic species,  $\text{Rh}_2\text{H}_2(\mu\text{-CO})_2(\text{et,ph-P4})]^{2+}$ , is formed *in situ* under  $\text{H}_2/\text{CO}$  pressure. This is one of the most impressive examples of homobimetallic cooperativity in homogeneous catalysis. The fragmentation of this catalyst by CO has been investigated and confirmed by *in situ* NMR spectroscopic studies. A new tetraphosphine ligand *rac*-*et,ph*-P4-Ph (*et,ph*-P4-Ph =  $\text{PEt}_2(o\text{-C}_6\text{H}_4)\text{P}(\text{Ph})\text{CH}_2(\text{Ph})\text{P}(o\text{-C}_6\text{H}_4)\text{PEt}_2$ ) has been synthesized to combat this fragmentation problem. However, the inability to successfully separate the *meso* and *racemic* isomers of the ligand has led to more alteration of the basic structure of the tetraphosphine ligands.

The current alteration being explored in an attempt to solve this separation problem is the replacement of the central methylene bridge by a tertiary amine. Experimentation has been conducted on the basis of a retrosynthetic analysis with the possibility of two pathways for formation of these aza-bridged ligands. The new ligands have not been afforded as of yet due to the difficulty in purification of the intermediate products. A simple Grignard-mediated phosphorus-carbon coupling reaction has been attempted with an amine bridge  $(\text{RN}(\text{PhPCI})_2$ , but impurities in the starting material and decreased reactivity of the amine bridge led to results that were undesirable. The second synthetic route relies upon coupling  $\text{PEt}_2(o\text{-C}_6\text{H}_4)\text{PPhCl}$  with a primary amine to afford the desired ligand, but the inability to obtain the pure phosphorus compound has hindered progress.

# Chapter 1: Hydroformylation

## 1.1. Introduction to Hydroformylation

Hydroformylation, also known as oxo synthesis, was discovered in 1938 by Otto Roelen while working at Ruhrchemie.<sup>1</sup> During his work on cobalt-catalyzed Fischer-Tropsch synthesis, he observed the conversion of ethylene, H<sub>2</sub>, and CO to propanal.<sup>1</sup> In the hydroformylation reaction, alkenes are converted to aldehydes when reacted with H<sub>2</sub>/CO (syngas) in the presence of a catalyst Scheme 1.1. Hydroformylation is the largest industrial homogenous process producing more than 15 billion pounds of aldehydes per year.

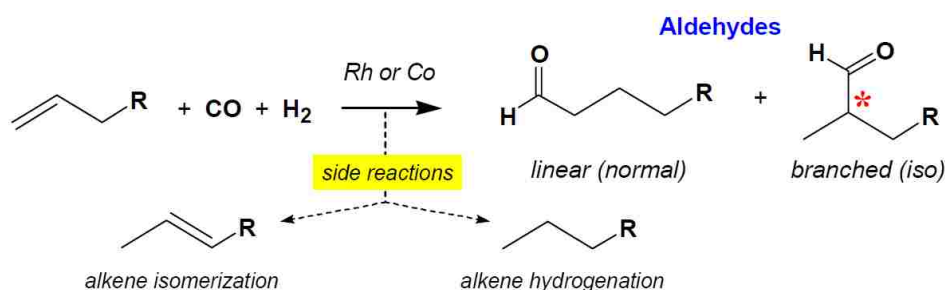


**Figure 1.1.** General hydroformylation reaction scheme.

Hydroformylation of  $\alpha$ -olefins results in two isomers of the aldehydes, linear (normal) and branched (iso). The linear aldehydes are used industrially for detergents and plasticizers. The branched aldehydes usually have a chiral carbon alpha to the aldehyde that is important in the production of fine chemicals and drugs.<sup>2</sup> Figure 2.1 shows some reactions that are utilized commercially to yield fine chemicals from aldehydes.<sup>3</sup>

## 1.2. Cobalt Hydroformylation Catalysts

The first hydroformylation catalyst used by Roelen was the unmodified cobalt hydrido-carbonyl complex, HCo(CO)<sub>4</sub>. The conditions for the reaction are quite harsh with a 1:1 CO:H<sub>2</sub> pressure of 200-300 bar and a temperature of 200-250 °C. The regioselectivity of C<sub>2</sub>-C<sub>7</sub> 1-alkenes is 2-4:1 linear to branched aldehydes and decreases as the alkene length increases. In addition to the harsh conditions, the active cobalt catalyst, HCo(CO)<sub>4</sub>, and its precursor, Co<sub>2</sub>(CO)<sub>8</sub>, are rather toxic.<sup>3</sup>

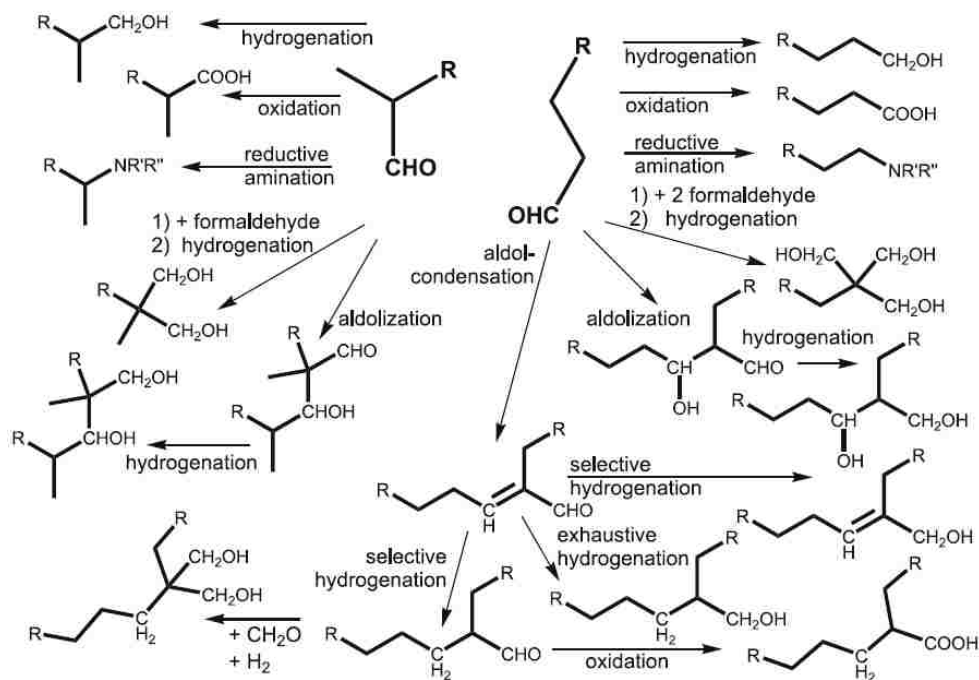


**Figure 1.2.** Commercially employed reactions of aldehydes.

It was not until 1961 that a widely accepted mechanism for cobalt-catalyzed hydroformylation was proposed by Heck and Breslow (Fig. 1.3).<sup>4</sup> The mechanism begins with hydrogenation of the bimetallic complex (**A**) to form the active monometallic cobalt hydride catalyst (**B**). The catalytic cycle begins with dissociation of CO and addition of the alkene substrate. This is followed by migratory insertion to form the alkyl species (**D**). A second migratory insertion occurs giving way to the acyl complex (**E**). A CO ligand dissociates then an oxidative addition of H<sub>2</sub> takes place. Reductive elimination gives the aldehyde product and the active catalyst is regenerated.

A modified-cobalt catalyst was developed by Slaugh and Mullineaux at Shell in 1968.<sup>5</sup> The use of trialkylphosphine to produce HCo(CO)<sub>3</sub>(PR<sub>3</sub>) as the active catalyst had dramatic effects on the rate, regioselectivity, and reaction conditions. The H<sub>2</sub>/CO pressure decreased to 50-100 atm and the temperature could be increased without decomposition of the catalyst at these lower pressures. Hydrogenation of the alkenes to alkanes is an undesirable side reaction that ranges from 10-20%.

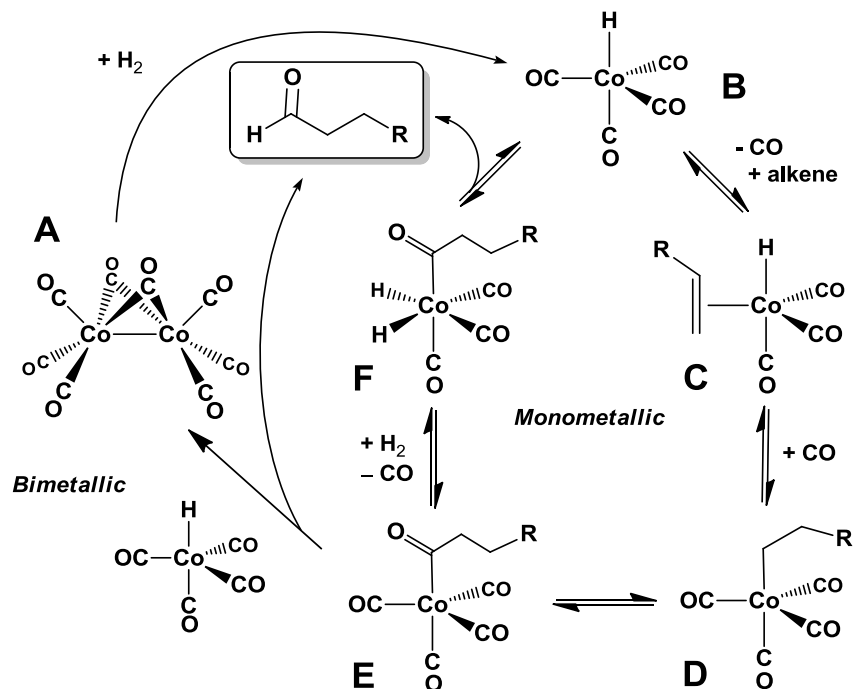


**Figure 1.3.** Heck-Breslow cobalt-catalyzed hydroformylation mechanism.

The selectivity of the linear to branched aldehyde ratio increased from 2-4:1 to 7-8:1 with the addition of the sterically directing alkylphosphine ligand. The reaction rate did suffer by being 5-10 times slower than the unmodified catalyst, but the increase in selectivity for the linear aldehyde product is more important to Shell for the detergents and surfactants that they produce.

### 1.3. Rhodium Hydroformylation Catalysts

In the late 1960's, Wilkinson and coworkers made a landmark discovery with the use of a modified rhodium catalyst,  $HRh(CO)(PPh_3)_2$ , for hydroformylation.<sup>7</sup> This phosphine rhodium  $H_2/CO$ . The generally accepted mechanism for the  $PPh_3$ -modified rhodium catalyst was catalyst was found to be active under very mild conditions (70-100°C; 5-25 atm  $H_2/CO$ ) and even at ambient conditions (25°C; 1 atm  $H_2/CO$ ). The selectivity for the product varied with conditions (20:1 at 25°C, 1 atm  $H_2/CO$ ; 9:1 at 50°C, 1 atm  $H_2/CO$ ; 3:1 at 25°C, 80-100 atm proposed by Wilkinson and is shown in Figure 1.4.

The rhodium-catalyzed hydroformylation mechanism begins with dissociation of a CO ligand and coordination of the alkene substrate to the unsaturated rhodium-hydride complex. This is followed by a migratory insertion of the alkene into the hydride-rhodium bond to form the alkyl species. Oxidative addition of H<sub>2</sub> occurs and the aldehyde product is reductively eliminated to reform the unsaturated rhodium-hydride species.

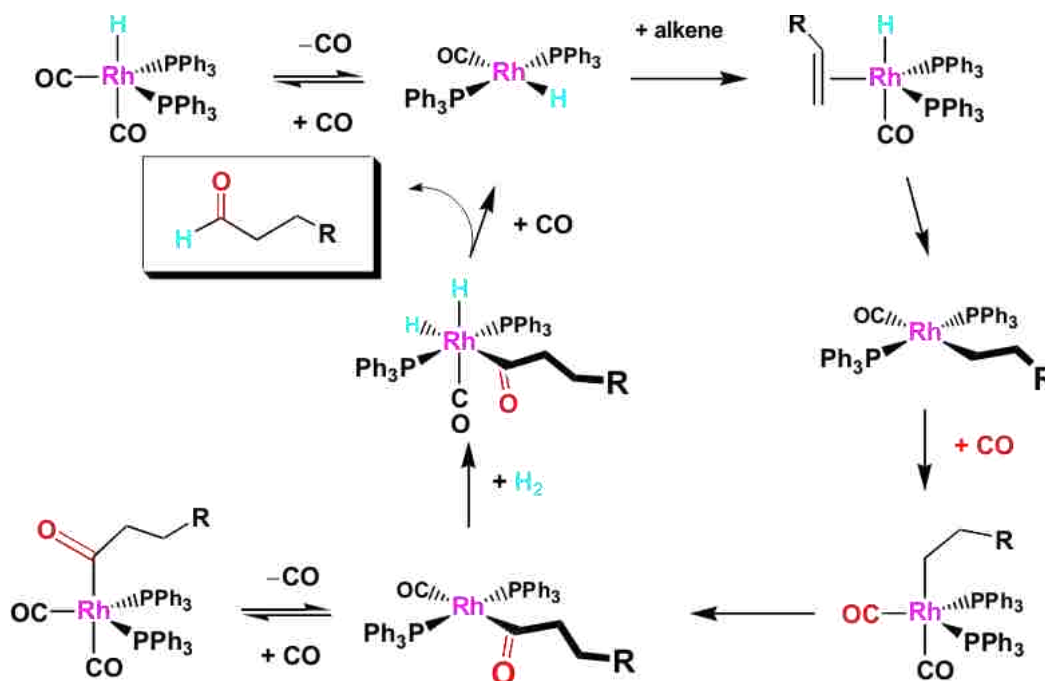


**Figure 1.4.** Proposed mechanism for rhodium-catalyzed hydroformylation.

The work of Pruet and Booth and coworkers led to the commercialization of modified-rhodium catalyzed hydroformylation. They discovered that the addition of excess  $\text{PPh}_3$  created a commercially viable catalyst system at 125-150 psig and 100-125 °C.<sup>6</sup> Excess phosphine ligand is necessary to stabilize the rhodium catalyst in order to inhibit the formation of an unsaturated 14 electron species. These species can lead to rhodium-induced phosphine fragmentation forming an alkyldiphenylphosphine ligand or bridged dirhodium complexes. With insufficient  $\text{PPh}_3$ , more active and less selective carbonyl-rich catalysts are formed. However, a very large concentration of  $\text{PPh}_3$  causes the hydroformylation reaction to be quite slow but has the highest selectivity to linear aldehyde.

#### 1.4. Mono- and Bis- Phosphine and Phosphite Ligands for Hydroformylation Catalysts

The original phosphine ligand for rhodium-catalyzed hydroformylation, triphenylphosphine ( $\text{PPh}_3$ ), used by Wilkinson and coworkers<sup>7</sup> showed far higher activity and regioselectivity than its cobalt predecessor. Modification of the “R” groups on the phosphine ( $\text{PR}_3$ ) and the use of phosphite ( $\text{P(OR)}_3$ ) ligands greatly influences the rate, regioselectivity, and stereoselectivity of the aldehyde product. Alterations of the R-groups on the ligands control the acceptor/donor ability and steric bulk of the ligands. Controlling the number of metal-bonding atoms, the bite angle, and the coordination geometry of polydentate phosphine/phosphite ligands are additional ways that the catalyst can be tailored.

In the mid-1970's, Chadwick Tolman developed methods to categorize the steric and electronic factors of a wide assortment of phosphine ligands. The results of his studies were published in 1977.<sup>8</sup> Although it can be difficult to separate electronic and steric effects, Tolman developed the system to quantify these effects in phosphine ligands, where they are very important.

The electronic parameter  $\chi$  (*chi*) is based on the carbonyl IR stretching frequencies based on  $\text{Ni(CO)}_3\text{L}_3$  compounds.<sup>9</sup> The electronic factors strongly influence the rate of hydroformylation catalysis. Electron donating ligands, such as alkylphosphines, on rhodium catalysts tend to slow the catalysis. The increased donation to the metal center causes more  $\pi$ -backbonding to occur, strengthening the metal-CO bonds, which causes the CO ligand to dissociate more slowly and generates saturated 18 e- complexes that can't coordinate alkene or  $\text{H}_2$ . Phosphite ligands, on the other hand, are generally poor  $\sigma$ -donors and moderately good  $\pi$ -acceptors. When used in hydroformylation  $\text{P(OR)}_3$  ligands usually generate extremely active catalysts, but often with lower regioselectivity. In most cases, phosphorus containing ligands increase the rate of rhodium catalyzed hydroformylation as follows: phosphites > arylphosphines (with electron-withdrawing substituents) > triphenylphosphine >

alkylphosphines.<sup>9</sup> Phosphite ligands decompose easily, which is another limiting factor in their use in hydroformylation catalysis.

The steric parameter  $\theta$  (*theta*) was developed because the presence of three R-groups allows for a remarkable degree of tailoring of the steric profile of the phosphine ligand. Also known as the Tolman cone angle, the steric parameter was initially based on space-filling CPK molecular models. The cone was constructed to embrace all substituents attached to the phosphorus atoms when the  $R_3P-M$  distance was 2.28 Å.<sup>9</sup> The steric bulk of the  $PR_3$  ligand dramatically affects the selectivity of the aldehyde product in hydroformylation catalysis. More bulky phosphine ligands favor the linear aldehyde product. However, the ligand can become too bulky, such as  $PCy_3$  (Cy = cyclohexyl) and the alkene substrate is not able to coordinate when two  $PCy_3$  ligands are bound to the Rh.

In 1981, Emily Kuntz, while at Rhone-Poulenc, developed a sulfonated- $PPh_3$  ligand,  $P(Ph-m-SO_3^-Na^+)_3$  (tppts) (Fig. 1.5). The rhodium catalyst that was formed,  $HRh(CO)[P(Ph-m-SO_3^-Na^+)]_3$ , was very soluble in water (1 kg ligand/1 kg water). This discovery led to a biphasic hydroformylation system that was commercialized by Ruhrchemie.<sup>9</sup> Due to the insolubility of longer chain alkenes in water, this system is only viable for the hydroformylation of propene and butene. In the early-to-mid 90's, Herrmann and coworkers prepared several other sulfonated

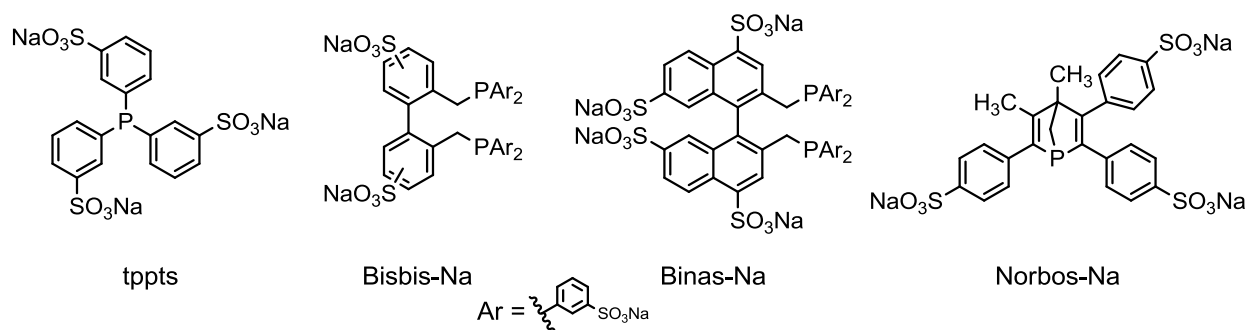


**Figure 1.5.** Various ligands used in biphasic hydroformylation.

ligands, Bisbis-Na, Norbos-Na, and Binas-Na, for biphasic hydroformylation (Fig. 1.5).<sup>10</sup>

Catalysts containing these ligands had greater activities than tppts (tppts = 1; Bisbis-Na = 5.6,

Norbos-Na = 7.4, and Binas-Na = 11.1). The regioselectivity of the Bisbis-Na and Binas-Na were also quite impressive at 32:1 and 49:1 linear to branched ratio respectively.

Phosphite ligands are better  $\pi$ -acceptors than phosphine ligands. This means that the rate of formation of the product will be increased due to the faster dissociation of the CO ligand, which is generally the rate determining step for the catalytic cycle. In 1969, Pruet and Smith reported triphenylphosphite and several ortho-substituted triphenylphosphite ligands for the hydroformylation of 1-octene and methyl methacrylate.<sup>6</sup> Van Leeuwen and Roobeek<sup>11</sup> discovered that the use of a bulky monophosphite ligand in the hydroformylation of relatively unreactive alkenes proceeded with high reaction rates. They also determined through their efforts that the selectivity for the linear aldehyde increased as the electron withdrawing nature of the ligands increased. Phosphite ligands are often used for the hydroformylation of unreactive alkenes if regioselectivity is not an issue. These include tributene,<sup>12a</sup> di- and tricyclopentadiene,<sup>12b</sup> and methacrylic acid alkyl esters.<sup>12c</sup> They are also used in the hydroformylation of internal alkenes due to fast isomerization of the double bond. Phosphite ligands are much easier to synthesize relative to phosphines (alkyl or aryl). Their downfall lies in the fact that they are far more likely to undergo hydrolysis and fragmentation reactions leading to limited catalyst lifetimes (turnover numbers).

The bisphosphites in Figure 1.6 were reported as early as 1956,<sup>13</sup> but were not introduced as ligands for hydroformylation until 1987 by Bryant and coworkers.<sup>14</sup> A low ligand to metal ratio has to be used because of the bulkiness and chelating nature of these ligands. Too high of a ligand:metal ratio would cause the catalyst to deactivate. These rhodium-bisphosphite catalysts were able to achieve a 95% linear-to-branched selectivity with 1-alkenes at 100 °C and 20 bar. This is a much larger than the 70% linear-to-branched ratio of the bulky monophosphite ligands.

The development of the bisphosphine ligand BISBI (Fig. 1.7) by Tom Devon at Texas Eastman<sup>15</sup> marked another significant ligand development in hydroformylation catalysts. This



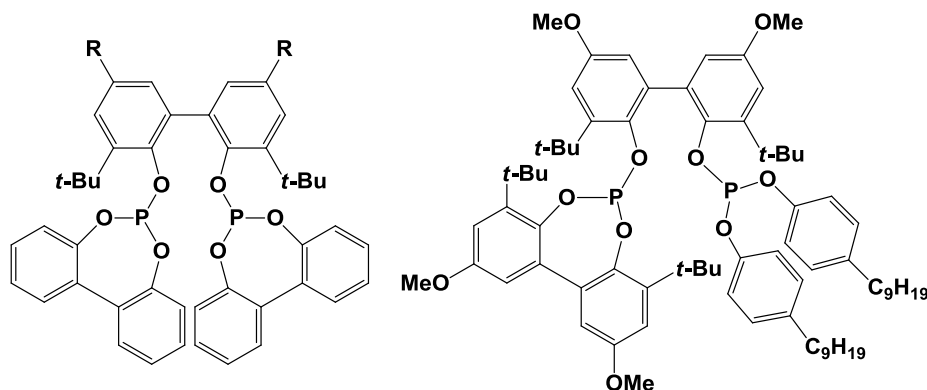


**Figure 1.6.** Bulky bisphosphite ligands.

ligand gave exceptional selectivity for the linear aldehyde product (30:1 l:b for propene). Investigation into the activity of the BISBI ligand led to the discovery of backbone and bite angle effects of bisphosphine ligands. These effects were studied by Casey and Whiteker<sup>16</sup> by comparing BISBI to other chelating bisphosphine ligands. They developed the idea of the natural bite angle ( $\beta_n$ ) which is “the preferred chelation angle, determined only by ligand backbone constraints and not by metal valence angles.” The natural bite angles were determined by molecular mechanics calculations. Through their studies, Casey and Whiteker determined that the high regioselectivity toward the linear product was attributed to the preferred equatorial-equatorial bisphosphine coordination on the catalytically active species,  $[\text{HRh}(\text{diphosphine})(\text{CO})_2]$ . The equatorial-equatorial bonding mode occurs because of BISBI's large bite angle, 113°.

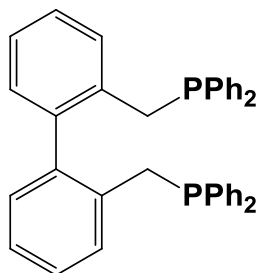


**Figure 1.7.** BISBI; Introduced to hydroformylation by Tom Devon.

In 1990, Prof. Piet van Leeuwen, at the University of Amsterdam, began investigating ligands with bite angles larger than 99°.<sup>17</sup> The series that were synthesized are known as

Xantphos ligands (Fig. 1.8) because the backbone is based on the organic heterocyclic compound xanthene. The bite angles of the series range between 102° and 121°. The catalysts formed with these ligands proved to be very selective for the linear aldehyde, with benzylnixantphos giving linear-to-branched ratios as high as 70:1. Through the work of Kranenburg<sup>18</sup> and Van der Veen,<sup>19</sup> it was shown that the general trend for the Xantphos-based rhodium catalysts was an increased linear-to-branched ratio and rate with increasing bite angle. However, they did find that once the bite angle grew too wide, the trend diminished.

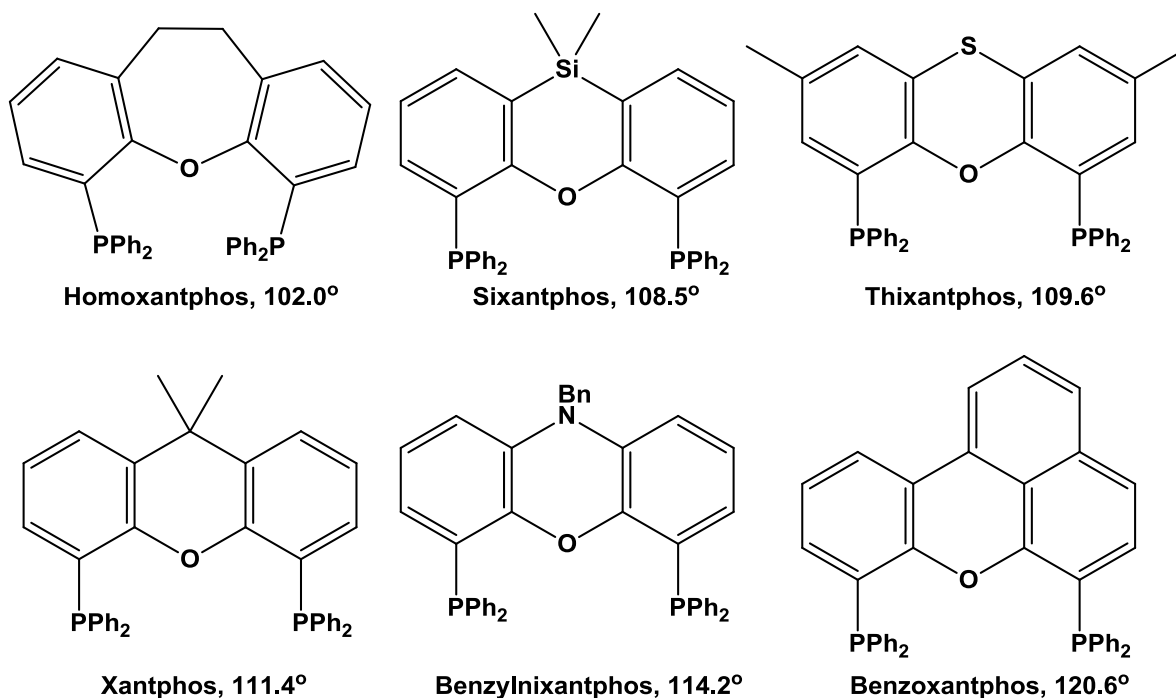


**Figure 1.8.** Examples from the Xantphos series and their calculated natural bite angles.

## 1.5. References

1. Cornils, B.; Hermann, W. A.; Rasch, M. *Angew. Chem., Int. Ed. Engl.* **1994**, *33*, 2144.
2. Yamashita, M.; Nozaki, K. Hydroformylation, Other Hydrocarbonylation, and Oxidative Alkoxycarbonylation. In *Comprehensive Organometallic Chemistry III*; Crabtree, R. H.; Mingos, D. M. P., Ed.; Elsevier: 2007; Vol. 11; p 436.
3. Wiese, K. D.; Obst, D., *Top. Organomet. Chem.* **2006**, *18*, 1.
4. Heck, R. F.; Breslow, D. S., *J. Am. Chem. Soc.* **1961**, *83*, 4022.

5. L. H. Slaugh and R. D. Mullineaux, *J. Organomet. Chem.* **1968**, *13*, 469.
6. R. L. Pruett and J. A. Smith, *J. Org. Chem.* **1969**, *34*, 327.
7. Evans, D.; Osborn, A.; Wilkinson, G. *J. Chem. Soc. A* **1968**, 3133.
8. Tolman, C. A. *Chem. Rev.* **1977**, *77*, 313-348.
9. Leeuwen, P. W. N. M. v. *Homogeneous Catalysis: Understanding the Art*, Kluwer Academic Publishers: Dordrecht; Boston, 2004.
10. (a) Herrmann, W. A.; Kohlpaintner, C. W.; Bahrman, H.; Konkol, W. *J. Mol. Catal.* **1992**, *73*, 191. (b) Herrmann, W. A.; Kohlpaintner, C. W.; Manetsberger, R. B.; Bahrman, H.; Kottmann, H. *J. Mol. Catal. A* **1995**, *97*, 65. (c) Cornils, B.; Wiebus, E. *Recl. Trav. Chim. Pays-Bas.* **1996**, *115*, 211.
11. (a) Van Leeuwen, P. W. N. M.; Roobeek, C. F. *J. Organomet. Chem.* **1983**, *258*, 343. (b) Van Leeuwen, P. W. N. M.; Roobeek, C. F. Brit. Pat. 2 068 377, **1980** (to Shell); *Chem. Abstr.* **1984**, *101*, 191 142.
12. (a) OXENO (2003) WO 2003095402. (b) Mitsubishi (2003) JP 2003146931. (c) Kuraray (1995) JP 07258149.
13. Anschutz, L.; Marquardt, *CHBEAM* **1956**, *89*, 1119.
14. (a) UCC (1987) EP 214622. (b) UCC (1988) US 4769498.
15. Devon, T. J.; Phillips, G. W.; Puckette, T. A.; Stavinoha, J. L.; Vanderbilt, J. J., (to Texas Eastman), *U.S. Pat.*, 4,694,109, 1987 (*Chem. Abstr.*, **1988**, *108*, 7890).
16. (a) Casey, C. P.; Whiteker, G. T.; Campana, C. F.; Powell, D. R. *Inorg. Chem.* **1990**, *29*, 3376. (b) Casey, C. P.; Whiteker, G. T.; Melville, M. G.; Petrovich, L. M.; Gavney, J. A.; Powell, D. R. *J. Am. Chem. Soc.* **1992**, *114*, 5535.
17. Kamer, P. C. J.; van Leeuwen, P. W. N. M.; Reek, J. N. H. *Acc. Chem. Res.* **2001**, *34*, 895.
18. Kranenburg, M.; van der Burgt, Y. E. M.; Kamer, P. C. J.; van Leeuwen, P. W. N. M. *Organometallics* **1995**, *14*, 3081.
19. van der Veen, L. A.; Keeven, P. H.; Schoemaker, C. C.; Reek, J. N. H.; Kamer, P. C. J.; van Leeuwen, P. W. N. M.; Lutz, M.; Spek A. L. *Organometallics* **2000**, *19*, 872.

## Chapter 2: Bimetallic Cooperativity in Hydroformylation

### 2.1. Introduction

One of the first suggestions of bimetallic cooperativity in homogeneous catalysis was given by Heck in 1961 in his proposed mechanism for cobalt catalyzed hydroformylation.<sup>1</sup> Heck did not favor this idea due to the low concentration of each species, but suggested it as a possibility. In the bimetallic pathway,  $\text{HCo}(\text{CO})_4$  and  $\text{Co}(\text{acyl})(\text{CO})_4$  take part in an intermolecular hydride transfer to reductively eliminate the aldehyde product and form the starting bimetallic precursor of the active catalyst (Fig. 2.1).

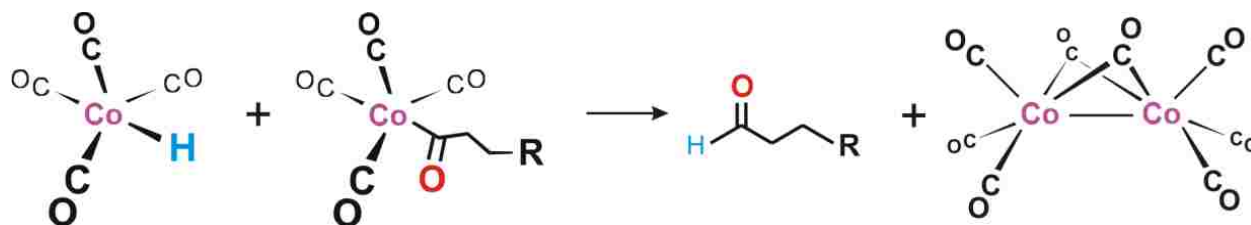


**Figure 2.1.** Proposed bimetallic pathway by Heck.

Polymetallic clusters were investigated as hydroformylation catalysts in hopes that they would have a synergistic effect when applied to the catalytic process. These types of catalysts tend to have drawbacks when used in hydroformylation catalysis. Pittman and coworkers reported the use of cobalt clusters, but they suffered from low linear-to-branched ratios (5:1 for 1-pentene) and the use of very high  $\text{H}_2/\text{CO}$  pressures (400-1100 psig).<sup>2</sup> Süss-Fink and coworkers reported a cluster catalyst  $[\text{HRu}_3(\text{CO})_{11}]^-$  with high regioselectivity (70:1 l:b) for the hydroformylation of propylene. The problem they encountered was the very low rate (55 TO in 66 h at 10 bar  $\text{H}_2/\text{CO}$ ).<sup>3</sup>

The use of a dirhodium thiolate-bridged catalyst was reported by Kalck in 1988 for the hydroformylation of 1-hexene.<sup>4</sup> The data presented by the authors showed a highly active and regioselective catalyst when  $\text{PPh}_3$  was added to the system. Kalck proposed the mechanism, which incorporates two intramolecular hydride transfers. However, studies on the system

performed by Southern<sup>5</sup> and van Leeuwen<sup>6</sup> have shown that the dirhodium species readily fragments and forms the active monometallic catalyst:  $\text{HRh}(\text{CO})_2(\text{PPh}_3)_2$ .

## 2.2. Discovery of a Cooperative Dirhodium Catalyst

Some of the best evidence of bimetallic cooperativity has been produced by Stanley and coworkers<sup>7</sup> with their dirhodium catalyst. Stanley uses a novel bridging and chelating tetraphosphine ligand, *meso*- and *rac*-*et,ph*-P4, to bind two rhodium centers via a conformationally flexible, methylene bridge to test the theory of bimetallic cooperativity in hydroformylation. The development of these ligands (Fig. 2.2) resulted in the formation of catalyst precursor *rac*- $[\text{Rh}_2(\text{nbd})_2(\text{et,ph-P4})](\text{BF}_4)_2$  (*nbd* = norbornadiene) by the reaction of *rac*-*et,ph*-P4 with 2 equivalents of  $[\text{Rh}(\text{nbd})_2]\text{BF}_4$  (Fig. 2.3). The *meso*-precursor is synthesized the same way using *meso*-*et,ph*-P4. A *meso*-catalyst is formed but the reactivity and selectivity are significantly lower than its *racemic* counterpart. Upon investigation, the *racemic* dirhodium active catalytic species, *rac*- $[\text{Rh}_2\text{H}_2(\mu\text{-CO})_2(\text{et,ph-P4})]^{2+}$ , has surpassed the rate and regioselectivity of most monometallic hydroformylation systems.

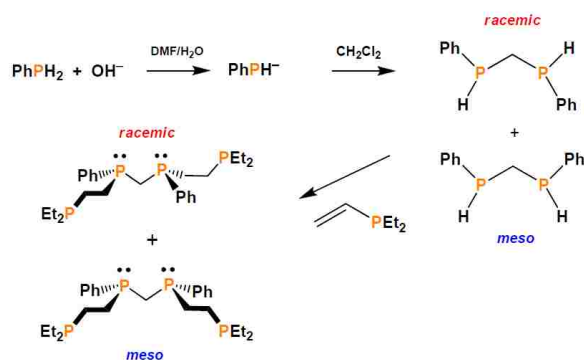


**Figure 2.2.** Synthesis of *meso* and *racemic* *et,ph*-P4.

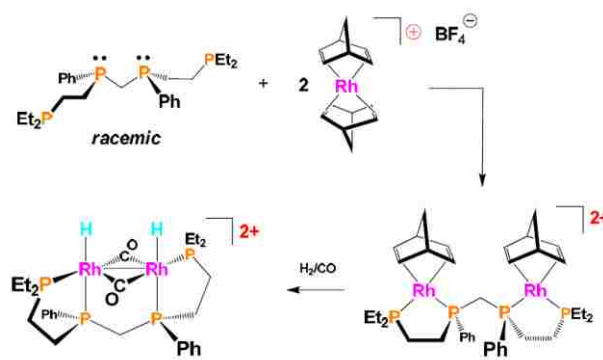


**Figure 2.3.** Synthesis of the catalyst precursor, *rac*- $[\text{Rh}_2\text{H}_2(\mu\text{-CO})_2(\text{et,ph-P4})]^{2+}$ .

There are several reasons for the increased rate and selectivity of the *racemic* version of the catalyst. The flexible methylene bridge allows the catalyst to exist in open- and closed- modes with (Fig. 2.4) rhodium-rhodium distances of 5-7 Å<sup>8a</sup> and <3 Å,<sup>8b</sup> respectively. The *racemic* species can more easily form the a closed-mode geometry with a lower energy edge-

sharing bioctahedral structure to facilitate the important intramolecular hydride transfer reaction steps. The *meso* species can perform the desired intramolecular hydride transfer, but it has more difficulty transforming to the closed-mode due to the two *cisoidal* chelating phosphine arms that limit the coordination environment around the Rh centers relative to the *racemic* ligand (Fig 2.5).

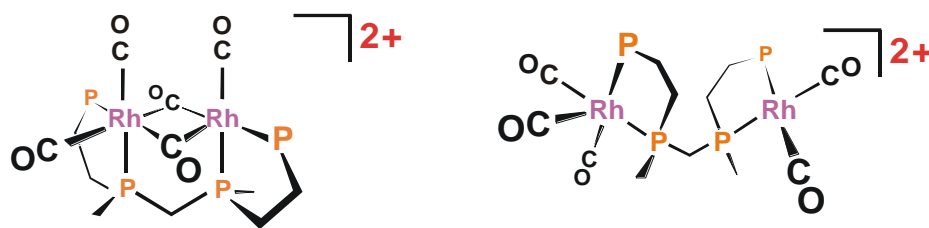


**Figure 2.4.** Open- and closed-mode dirhodium complexes.

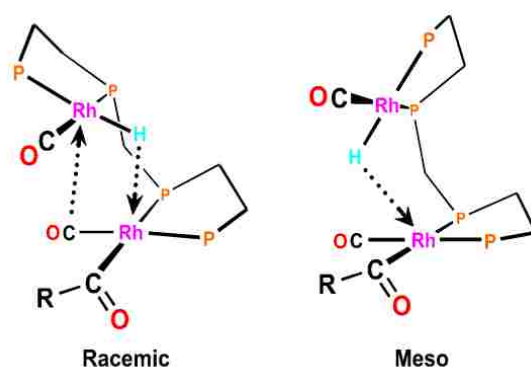


**Figure 2.5.** Intramolecular hydride transfer in *racemic* and *meso* catalysts.

The mechanism for the bimetallic hydroformylation proposed by Prof. Stanley is depicted in Figure 2.6. It begins with the open-mode pentacarbonyl complex **A** undergoing the oxidative addition of  $H_2$  to produce the mixed oxidation state complex **B**, with Rh(+1)/Rh(+3) centers. The first intramolecular hydride transfer occurs to form the active catalytic species (with two Rh(+2) centers) **D**, through the intermediate **C**. An open site for the alkene species to coordinate is formed by the dissociation of a terminal CO ligand to form complex **E**. A migratory insertion of the alkene into the hydride-Rh bond occurs to form complex **F**. A CO ligand coordinates to the open site and undergoes a migratory insertion into the alkyl-Rh bond to form **G**. At this point, the second intramolecular hydride transfer occurs to reductively eliminate the aldehyde product and

form complex **H**, which can then react with  $H_2$  to reform complex **C** or coordinate a CO ligand to produce the open-mode complex **A**.

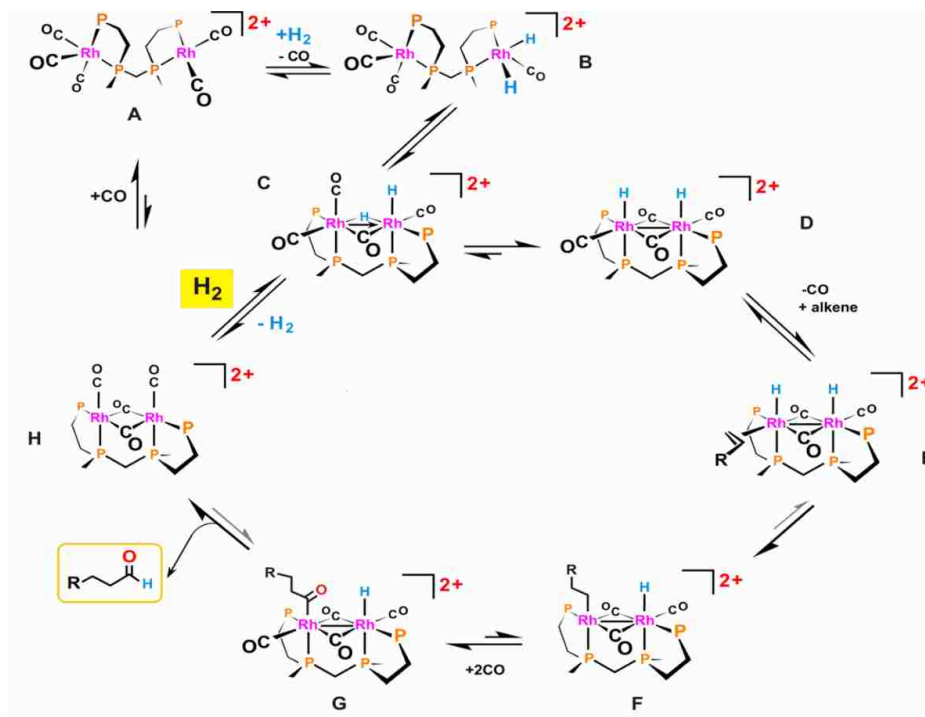


**Figure 2.6.** Stanley's proposed bimetallic hydroformylation mechanism.

### 2.3. Confirmation of Bimetallic Cooperativity

The first strong evidence of bimetallic cooperativity in Prof. Stanley's catalyst was that similar monometallic species tested ( $[Rh(nbd)(P_2)]BF_4$  where  $P_2 = Et_2PCH_2CH_2PEt_2$ ,  $Et_2PCH_2CH_2PMePh$ ,  $Et_2PCH_2CH_2PPh_2$ , or  $Ph_2PCH_2CH_2PPh_2$ ) were terrible hydroformylation catalysts. The results of these hydroformylation runs gave only 1-2 TO/h, 3:1 linear to branched product regioselectivity, and 50-70% alkene isomerization.<sup>7a, 9</sup>

To further test the theory of bimetallic cooperativity, the methylene bridge of *et,ph*-P4 was replaced by a "rigid" *p*-xylene and propylene bridges (Fig. 2.7). This forced the rhodium centers to be spaced far enough to stop or hinder interaction with one another. These analogs of the *et,ph*-P4 ligand also resulted in extremely poor hydroformylation catalysts, with results

similar to the previously tested monometallic catalysts (0.5-6 TO/h, 3:1 l:b product regioselectivity, 50-70% alkene isomerization, and hydrogenation side reactions).<sup>7a, 9</sup>

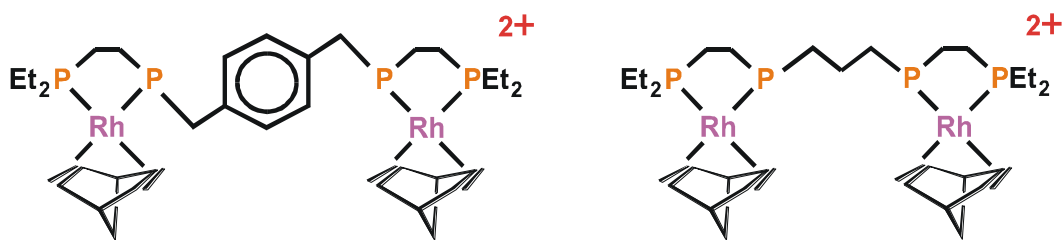


**Figure 2.7.** Spaced bimetallic analogs.

#### 2.4. Polar-Phase Hydroformylation

The initial results published for Stanley's hydroformylation catalyst, *rac*-[Rh<sub>2</sub>(nbd)<sub>2</sub>(et,ph-P4)]<sup>2+</sup>, were very impressive. As shown in Table 2.1, the *racemic* catalyst was more than double the rate and over 1.5 times more selective than the industrially used Rh/PPh<sub>3</sub> system. The *meso*-[Rh<sub>2</sub>(nbd)<sub>2</sub>(et,ph-P4)] species was far less active and selective than its *racemic* counterpart with many more side reactions.<sup>7a</sup>

**Table 2.1.** Hydroformylation\* of 1-hexene.

Catalyst (or Precursor)	Initial TOF (hr <sup>-1</sup> )	L:B	Iso	Hydro
<i>rac</i> -[Rh <sub>2</sub> (nbd) <sub>2</sub> (et,ph-P4)]	1200	25:1	2.5%	3.4%
HRh(CO)(PPh <sub>3</sub> ) <sub>2</sub> (0.8M PPh <sub>3</sub> )	540	17:1	1%	<0.1%
<i>meso</i> -[Rh <sub>2</sub> (nbd) <sub>2</sub> (et,ph-P4)]	55	14:1	24%	10%

\*90 psig 1:1 H<sub>2</sub>/CO; 90 C; 1 mM catalyst; 1 M 1-hexene (1000 equivalents); acetone solvent.

These catalytic runs were performed in acetone as the solvent. The catalyst performed very well in this solvent but it, like most homogeneous catalysts, was difficult to separate from the product. Since the aldehyde product is non-polar, a polar phase was added to the solvent system in hopes that the aldehyde product would separate and allow the catalyst to remain in the water/acetone layer. With the addition of a 30% water/acetone solvent system, an increase



in the activity (initial TOF  $20 \text{ min}^{-1}$  to  $30 \text{ min}^{-1}$ ) and selectivity (l:b 25:1 to 33:1) were observed. This shift to a water/acetone solvent increased the rate of hydroformylation by [*rac*-Rh<sub>2</sub>(μ-CO)<sub>2</sub>(et,ph-P4)]<sup>2+</sup> by 50%, increased the l:b aldehyde selectivity to 33:1, and reduced side reactions to less than 0.5%. 30% water (by volume) in acetone also greatly increased the lifetime of the dirhodium catalyst. Initially in the acetone solvent at 90 °C and 90 psig H<sub>2</sub>/CO, the catalyst was completely deactivated within 80 minutes. In the water/acetone solvent system under the same conditions, a mere 10% deactivation of the catalyst was observed after 2 hours. Unfortunately, the use of the polar phase solvent did not solve the catalyst/product separation problem because the dirhodium catalyst is more soluble in the aldehyde product than the water-acetone solvent.<sup>10</sup>

## 2.5. H<sub>2</sub>/CO Ratio Studies

Dr. Bobby Barker initially studied the effect of varying H<sub>2</sub>/CO ratios and pressures in the dirhodium catalyst system.<sup>11</sup> From *in situ* spectroscopic studies and hydroformylation runs at higher pressures, it was believed that CO played a major role in the fragmentation of our catalyst (see Chapter 3 for more detail). Due to the lack of literature on this type of study, Barker performed the H<sub>2</sub>/CO studies on our catalyst and several monometallic catalysts. His results showed that changing H<sub>2</sub>/CO pressure and ratio had a remarkable effect on our catalyst. As shown in Table 2.2, increasing the H<sub>2</sub>/CO ratio greatly increases the selectivity of the aldehyde product. The linear to branched ratio increased to 152:1 (99.3%) in the highest ratio studied. Barker found that decreasing the total pressure from 90 psig to 45 psig with a 1:1 H<sub>2</sub>/CO ratio caused an increase in the linear to branched selectivity from 33:1 (97.1%) to 55:1 (98.2%), although a 33% decrease in the rate was observed. For the subsequent studies, the CO partial pressure was kept at 22.5 psig and the H<sub>2</sub> partial pressure was increased the proper amount to give the desired H<sub>2</sub>/CO ratio. As the ratio was increased to 2:1 and 3:1, the linear to branched ratio increased to 64:1 (98.5%) and 75:1 (98.7%) respectively. At a 4:1 H<sub>2</sub>/CO ratio, the initial turnover frequency increased dramatically to 46 and the linear to branched ratio increased to an

**Table 2.2.** Rh<sub>2</sub> hydroformylation data from variable H<sub>2</sub>/CO ratio and pressure studies. Performed by Dr. Bobby Barker. Conditions: 90 °C, 1 M 1-hexene (1000 equiv.), 1 mM Rh catalyst, solvent = 30% H<sub>2</sub>O in acetone, constant pressure conditions, 1000 rpm stirring; pressures listed as psig, TOF = initial turnover frequency, TON = total turnover number, L:B = aldehyde linear to branched regioselectivity, Isom. = alkene isomerization. \* ca. 5% *n*-heptanol produced

H <sub>2</sub> /CO	pH <sub>2</sub>	pCO	TOF	TON	L:B	% linear	Isom
1:1	45.0	45.0	30(2)	1000	33:1	97.1	<1%
1:1	22.5	22.5	20(1)	1000	55:1	98.2	<1%
2:1	45.0	22.5	27(2)	1000	64:1	98.5	<1%
3:1	67.5	22.5	30(2)	1000	75:1	98.7	<1%
4:1	88.0	22.5	46(1)	1000	152:1	99.3	7.7%*
1:4	22.5	82.5	-	0	-	-	-
1:3	22.5	67.5	-	0	-	-	-

incredible 152:1 (99.3%). This great increase was accompanied by 7.7% isomerization and 5% hydrogenation of the aldehyde product.

A problem with Dr. Barker's studies was that the hydroformylation runs were done with fixed gas ratios in batch autoclaves. If you are feeding in a 3:1 H<sub>2</sub>/CO gas mixture, the hydroformylation catalysis is only consuming a 1:1 H<sub>2</sub>/CO stoichiometry. This leads to "left-over" H<sub>2</sub> and a steadily increasing H<sub>2</sub>/CO gas mixture ratio in the autoclave.

Dr. Catherine Alexander tried to get more dramatic results with increased gas ratios by doing 10,000 turnovers.<sup>12</sup> Unfortunately, the "left-over" H<sub>2</sub> "problem" causes very serious problems when trying to do more turnovers, leading to catalyst degradation and very poor results. This led to the true realization of the problems involved in running different gas ratios in our batch autoclaves. Dr. Alexander tried a host of experiments to initially charge the autoclave with the appropriate H<sub>2</sub>/CO gas mixture, then pressure add the 1-hexene substrate with a 1:1 H<sub>2</sub>/CO feed gas in order to maintain the appropriate gas ratio in the autoclave. Experimental difficulties led Dr. Alexander and Prof. Stanley to undertake a major redesign of the autoclaves to allow far easier assembly/disassembly and cleaning.

## 2.6. References

1. Heck, R.; Breslow, D. J. *J. Am. Chem. Soc.* **1961**, *83*, 4022.
2. Ryan, R. C.; Pittman, C. U., Jr. *J. Am. Chem. Soc.* **1977**, *99*, 1986.
3. Süss-Fink, G.; Schmidt, G. F. *J. Mol. Catal.* **1987**, *42*, 361.
4. Kalck, P. *Polyhedron* **1988**, *7*, 2441.
5. Davis, R.; Epton, J. W.; Southern, T. G. *J. Mol. Catal.* **1992**, *77*, 159.
6. Diéguez, M.; Claver, C.; Masdeu-Bultó, A. M.; Ruiz, A.; van Leeuwen, P. W. N. M.; Schoemaker, G. C. *Organometallics* **1999**, *18*, 2107.
7. (a) Broussard, M. E.; Juma, B.; Train, S. G.; Peng, W. J.; Laneman, S. A.; Stanley, G. G. *Science* **1993**, *260*, 1784. (b) Matthews, R. C.; Howell, D. K.; Peng, W.-J.; Train, S. G.; Treleaven, W. D.; Stanley, G. G. *Angew. Chem., Int. Ed. Engl.* **1996**, *35*, 2253.
8. (a) Laneman, S. A.; Fronczek, F. R.; Stanley, G. G., *Inorg. Chem.* **1989**, *28*, 1872. (b) Laneman, S. A.; Fronczek, F. R.; Stanley, G. G., *Inorg. Chem.* **1989**, *28*, 1206.
9. Broussard, M. E.; Louisiana State University (Baton Rouge La.). Dept. of Chemistry. Thesis (Ph D), Louisiana State University, Baton Rouge, 1993.
10. Aubry, D. A.; Bridges, N. N.; Ezell, K.; Stanley, G. G. *J. Am. Chem. Soc.* **2003**, *125*, 11180.
11. Barker, B. L.; Louisiana State University (Baton Rouge La.). Dept. of Chemistry. Thesis (Ph D), Louisiana State University, Baton Rouge, 2005.
12. Alexander, C. L. T.; Louisiana State University (Baton Rouge La.). Dept. of Chemistry. Thesis (Ph D), Louisiana State University, Baton Rouge, 2009.

## Chapter 3: Design and Synthesis of Aza-Bridged Tetrphosphine Ligands

### 3.1. Introduction

Although our catalyst is very active and very selective toward hydroformylation of alkenes, it suffers from fragmentation problems. Generally speaking, fragmentation and decomposition can lead to catalyst deactivation and is a very common problem. Oxidation of the phosphorus ligands is one source of catalyst decomposition. This can be limited through the careful removal of oxygen and hydroperoxides from substrates, solvents, and equipment. Ligand oxidation can also be avoided by adding excess ligand to the reaction mixture, as in the Rh/PPh<sub>3</sub> hydroformylation system. Unfortunately for our dirhodium tetrphosphine catalyst, the work of Monteil<sup>1</sup> demonstrated that the addition of excess PPh<sub>3</sub> causes a dramatic decrease in the rate and selectivity of hydroformylation. As the concentration of PPh<sub>3</sub> increases, the catalyst activity continues to decrease until it is almost completely inhibited. Due to these results, the addition of excess PPh<sub>3</sub> or et<sub>3</sub>ph-P4 to inhibit ligand oxidation is not an option for our catalyst system.

Fragmentation of monometallic rhodium-phosphine catalysts usually occurs in one of three ways: 1) oxidative addition of a P-C bond to the Rh center, 2) nucleophilic attack on a coordinated phosphine, and/or 3) ortho-metallation.<sup>2</sup> Oxidative addition of a P-C bond to the Rh center can lead to the formation of stable rhodium clusters with phosphide-bridges that are inactive for hydroformylation (Fig. 3.1a). Alternatively, a less active rhodium-phosphine catalyst can be formed by reductive elimination of a Rh-alkyl and the diphenylphosphide group. This forms a diphenylalkylphosphine ligand which is less sterically directing, leading to lower linear-to-branched aldehyde regioselectivities, and a stronger electron donor than the starting PPh<sub>3</sub> (Fig. 3.1b), which generates a less active catalyst. Ortho-metallation, also known as an intramolecular C-H oxidative addition, occurs with activation of the ortho-carbon-hydrogen bond. The ortho-C-H initially coordinates to the electron-rich metal center and does a C-H oxidative

addition to form a 4-membered metallocycle (Fig. 3.1c), which is a poor catalyst. Lastly, nucleophilic addition to the coordinated phosphorus atoms can occur if nucleophiles are present in the reaction mixture. The nucleophiles that are known to readily perform this attack are acetate, methoxy, hydroxyl, and hydride (Fig. 3.1d).

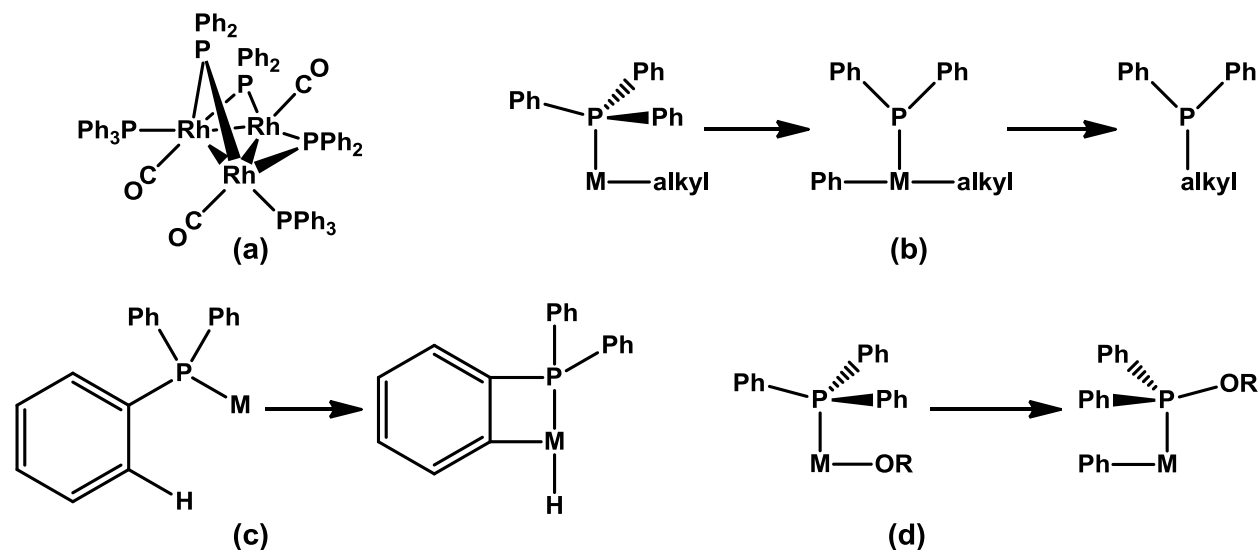


**Figure 3.1.** Routes to ligand decomposition.

Our dirhodium catalyst's "fragmentation" is *not* attributed to the same causes as the monometallic rhodium species with triarylphosphine ligands. Prof. Stanley has proposed the mechanism for the decomposition of our Rh<sub>2</sub>-catalyst shown in Figure 3.2, which is based on 1D and 2D <sup>31</sup>P NMR, <sup>1</sup>H NMR, and HMBC spectra.

Due to the flexibility of the external phosphine arms, it is proposed that **1** and **A** are in equilibrium. Both **1** and **A** are active for hydroformylation, with **A** being less selective due to the decrease in steric hindrance for incoming alkenes. Higher CO partial pressures lead to the formation of **A** which puts the catalyst on a path of decomposition. Conversely, increasing the H<sub>2</sub> partial pressure favors the formation of **1**, leading to a higher I:b ratio in product formation. The replacement of a donating PR<sub>3</sub>-donor with a π-back-bonding CO to form **A** makes the Rh more electron-deficient. This deficiency, in turn, favors the reductive elimination of H<sub>2</sub> to form **B**, which can lose a rhodium center to form **C**. At this point **C** can either react with another

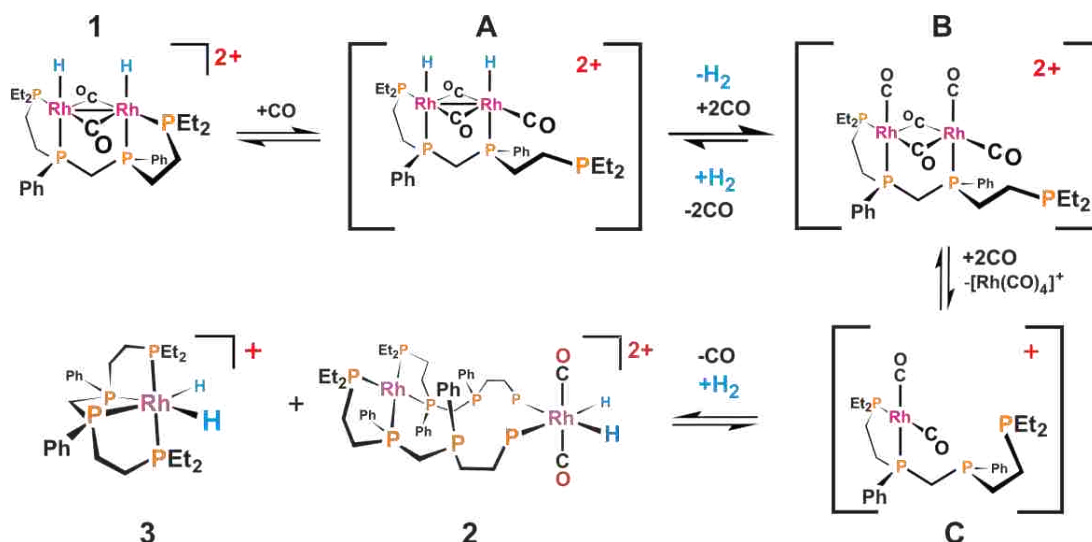


**Figure 3.2.** Proposed fragmentation pathway for the dirhodium catalyst.

molecule of **C** to form **2** (currently proposed preliminary structure), or the et,ph-P4 ligand can wrap around one rhodium center to form **3**. Both complexes, **2** and **3**, are very poor hydroformylation catalysts. Prof. Stanley believes that **2** is responsible for the alkene isomerization and hydrogenation side reactions seen.

### 3.2. Evolution of the P4 Ligand

This proposed fragmentation problem motivated Prof. Stanley to design a new ligand that would have a more rigid framework using *o*-phenylene linked arms to hold the external phosphines in closer proximity to the metal center. We call this ligand et,ph-P4-Ph, or P4-Ph (Fig. 3.3). Using a 1,2-disubstituted phenylene bridge instead of the rotationally more flexible ethylene groups in the P4 framework should generate an extremely strong chelating bisphosphine unit.

The synthetic scheme to build this ligand was designed by Dr. Alex Monteil (Fig. 3.3)<sup>1</sup> and features Mg-I exchange reactions. A slight modification has been made in which 1,2-diiodobenzene has been replaced by 1-bromo-2-iodobenzene to ensure that the first reaction of (iPr)MgBr and the aryl halide only occurs at one site - the more reactive iodide - on the benzene ring to decrease the chance of byproducts. All attempts to separate the *meso*- and *racemic*

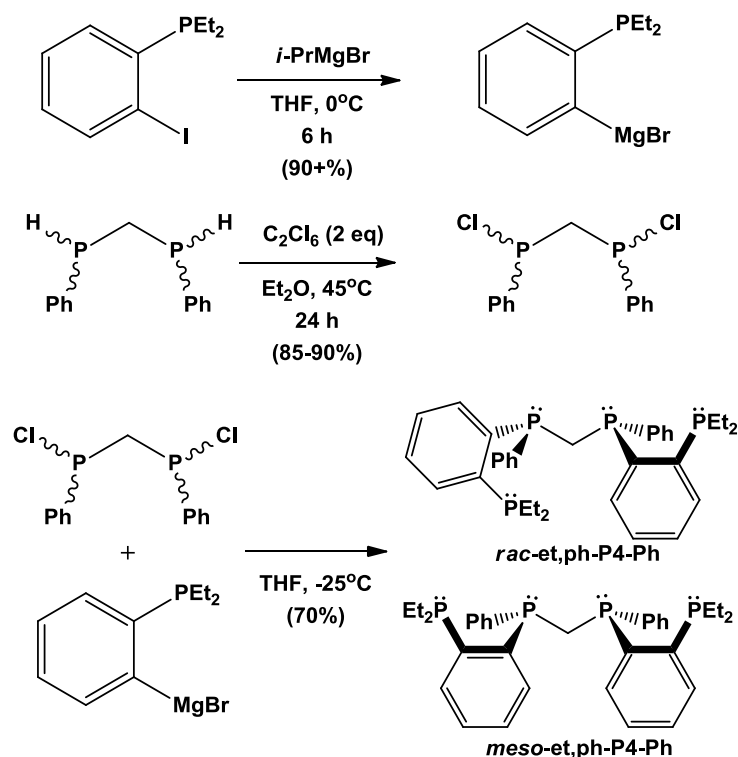


**Figure 3.3.** Synthetic scheme for the et,ph-P4-Ph ligand.

isomers of the P4-Ph ligand have been, so far, unsuccessful. Marc Peterson, of the Stanley group, attempted to make derivatives of the P4-Ph ligand by adding different groups onto the para position on the internal phenyl rings (Fig. 3.4). This was done in hopes of achieving the desired separation of the *racemic* and *meso*- isomers of the ligand by recrystallization. He had success in forming the  $-\text{NMe}_2$  and  $-t\text{-Bu}$  para-substituted primary halophosphines (83% yield).

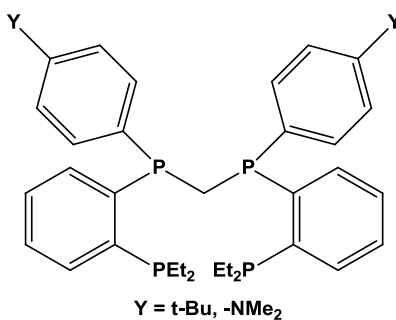


**Figure 3.4.** Et,ph-P4-Ph with para-substituted internal phenyl rings.

Reduction of these compounds to the primary phosphines was attempted with lithium aluminum hydride, but only the phenylphosphine ring with the *t*-Bu moiety could be reduced. Having

accomplished this, the next step was to form the bisphosphine bridge. The overall yield for the synthetic scheme was extremely low (9%) so higher yield routes to this general ligand framework are still needed.

The next step of ligand evolution comes in the form of “PNP” type ligands. Prof. Stanley suggested that replacing the methylene bridge with a tertiary amine bridge might allow an easier isomer separation (Fig. 3.5). It could also simplify the synthesis due to higher yielding routes to P-N(R)-P bridges.

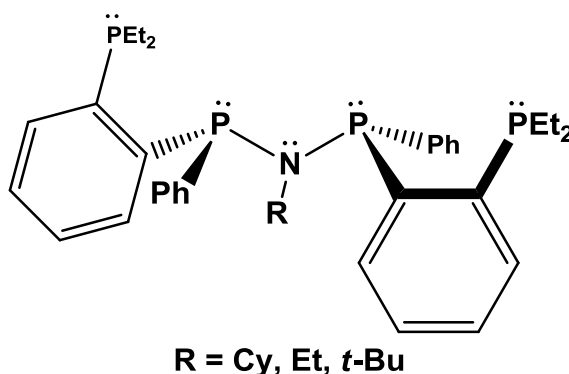


**Figure 3.5.** The new aza-bridged et,ph-P4-Ph ligand.

### 3.3. Changes in the Catalyst by Ligand Variation

#### 3.3.1. The et,ph-P4 Ligand

The original tetraphosphine ligand, et,ph-P4, is a coordinating ligand that strongly binds to the metal centers. Normally, an alkylated phosphine ligand is too strong a  $\sigma$ -donor to use successfully in rhodium-catalyzed hydroformylation. It causes the CO ligands to bond too strongly to the rhodium centers because of the increased electron density on the metal center and increased  $\pi$ -backdonation to the CO ligands. Dissociation of a CO ligand is vital to allow a saturated 18-electron complex to form a reactive 16-electron complex allowing coordination of the alkene or H<sub>2</sub>. To allow facile dissociation of a CO ligand, the strong donor ability of the P4 ligand is compensated by having a dicationic dirhodium catalyst, in which each Rh centers is in the +2 oxidation state.<sup>3</sup>



### 3.3.2. The et,ph-P4-Ph (aka P4-Ph) Ligand

The new et,ph-P4-Ph is a weaker  $\sigma$ -donor/better  $\pi$ -acceptor due to the ethylene linkages being replaced by mildly electron-withdrawing ortho-phenylene linkages. This should decrease the electron density on the rhodium centers allowing for faster dissociation of CO ligands. More electron deficient metal centers typically lead to a more active hydroformylation catalyst. Regioselectivity of the product should not be a major concern with the P4-Ph ligand because our catalyst containing the et,ph-P4 is not subjective to the normal distortion of monometallic catalysts upon alkene addition due to the rigid structure enforced by the ligand, Rh-Rh bonding, and bridging CO ligands. The closer proximity of the external phosphorus atoms to the metal centers caused by the ortho-phenylene linkages may not completely inhibit dissociation of the arms due to the decreased donor ability of all the phosphorus atoms of the ligand, but it should coordinate orders of magnitude more strongly than our first generation et,ph-P4 ligand.

### 3.3.3. The RN-P4-Ph Ligands

Replacing the methylene bridge with an amine bridge can have electronic and steric effects on the catalyst. The flexibility of the bridge should change a little due to the amine's ability to adopt a trigonal planar geometry. Peterson and coworkers<sup>4</sup> performed an *ab initio* study comparing diphosphinomethane (dpm) and diphosphinoamine (dpa). It showed that the optimal central angle for dpm is 113° while the optimal angle for dpa is 122° as it adopts a trigonal planar geometry ( $sp^2$  hybridized N atom). These calculations are in agreement with solid state structures of bis(diphenylphosphino)amine (dppa) and bis(diphenylphosphino)methane (dppm). The tension placed on the ligand when chelating a single metal due to the larger natural central angle of the PNP-ligand may explain why these ligands have a stronger tendency to bridge two metal centers rather than chelate a single metal center. The central angle for dpa, 122°, is closer to the angle needed to bridge two metal centers, 125°-130°. Conforming to this "ideal" bridging geometry only requires a 1.3 kcal mol<sup>-1</sup> distortion for dpa, while 5.6 kcal mol<sup>-1</sup> is required for dpm. Favoring binuclear coordination is exactly what we want for our catalyst, since

one of the fragmentation pathways leads to a chelated and thermodynamically very stable mononuclear complex (see Figure 3.2). The ability to easily add a wide variety of central R groups to the N-atom of the PNP ligand is also a big advantage that we do not have with the P-CH<sub>2</sub>-P-based ligands. Adding a bulkier group to the central N-atom could favor closed-mode bimetallic structures that we believe are important in catalysis.

These PNP ligands can also be tuned to favor chelation. Recently, Butcher and coworkers<sup>5</sup> have reported diphosphazanes with bulky groups attached to the phosphorus atoms, EtN[P(OR)<sub>2</sub>]<sub>2</sub> (R = -C<sub>6</sub>H<sub>3</sub><sup>i</sup>Pr<sub>2-2,6</sub> and C<sub>6</sub>H<sub>3</sub>Me<sub>2-2,6</sub>). These bulky groups cause a decrease in the central PNP bond angles to bring them closer to the angles needed to chelate one metal center, 109.5° and 113.1° respectively. The phenyl rings on the internal phosphorus atoms can be substituted in the ortho positions with methyl, ethyl, or isopropyl substituents to possibly decrease the PNP angle.

Adding the amine bridge will cause the internal phosphines to be better electron donors than the methylene bridged phosphines, and the alkyl group attached to the amine can be altered to tailor the donation of the internal phosphines. This added donor tunability could be used, if necessary, to combat some of the decrease in the donation caused by the ortho-phenylene linkages.

As stated previously, the *racemic* ligand is the desired form and makes the active catalytic species. Norman and coworkers reported 9-12:1 *meso:racemic* ratio for the synthesis of i-PrN[PhP(i-PrNH)]<sub>2</sub>.<sup>6</sup> Our normal et,ph-P4 ligand racemizes at 120°C to give a 48%/52% *meso/racemic* mixture after approximately 12 hours. The new PNP ligands may not be able to withstand these temperatures which could lead to decomposition of the ligand. This might pose a serious problem in ligand synthesis if we cannot obtain a good quantity of the *racemic* ligand.

Replacement of the methylene bridge with an amine bridge can cause significant changes in the coordination and structural features of the formed complexes. With suitable substituents on the P and N atoms, these ligands can stabilize metal-metal bonds, which we

believe is important in our hydroformylation catalysis. A review by Balakrishna *et al.* highlights a large variety of PNP- $M_x$  complexes.<sup>7</sup> As seen in Figure 3.6, PNP ligands can cause formation of clusters, bridged species without M-M bonds, bridged species with multiple metal-metal bonds, and metal centers containing bidentate and monodentate ligands.

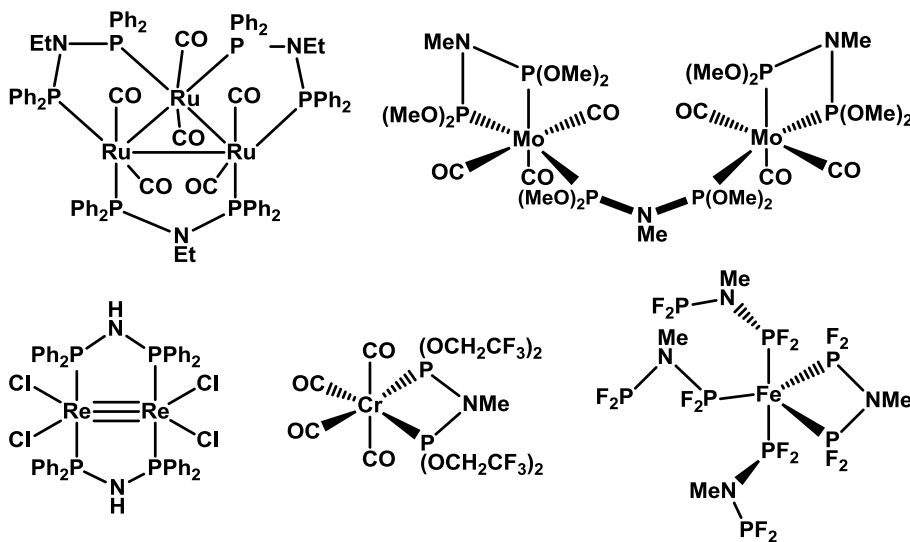


**Figure 3.6.** Some examples of PNP-metal complexes.

### 3.4. Fragmentation and Side Reactions of PNP Ligands

Several problems may arise with the use of PNP ligands. These ligands are susceptible to metal assisted cleavage when complexed with transition metals to give undesired products (Fig. 3.7).<sup>8</sup> Cleavage of a P-N bond can lead to iminophosphane type bridging ligands that donate to the metal centers through the phosphorus and nitrogen of the fragmented ligand and a separate bridging phosphide ligand.

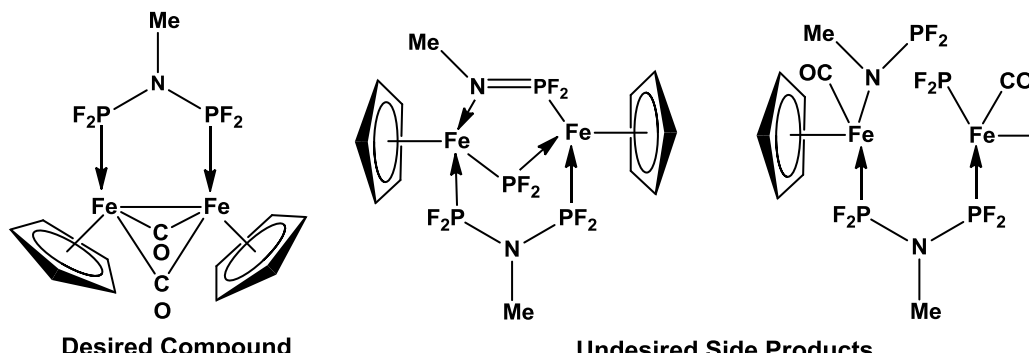


**Figure 3.7.** Some examples of metal assisted cleavage of PNP ligands.

It has recently been reported that the reaction of P(III)-N bonds of PNP compounds with aldehydes can lead to phosphine oxidation accompanied by C-insertion into the P-N bond or formation of  $\alpha$ -hydroxy phosphine oxides.<sup>9</sup> As seen in Figure 3.8, when bis(diphenyl-

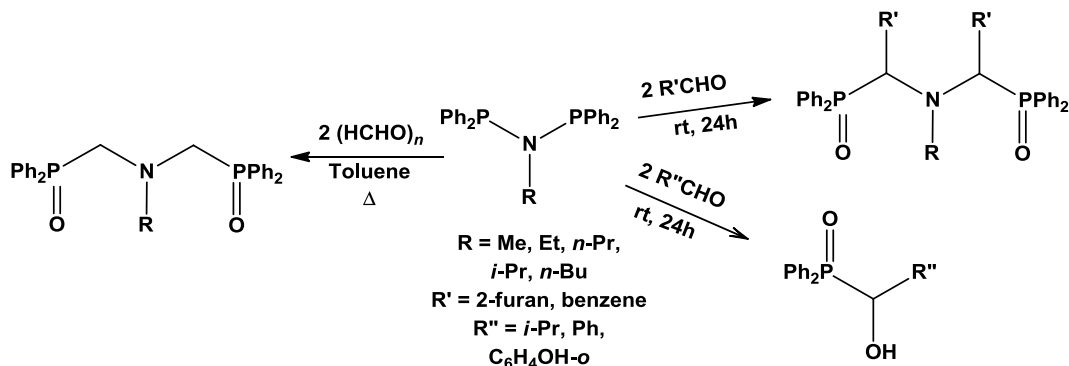


**Figure 3.8.** Fragmentation of PNP ligands via reaction with aldehydes.

phosphino)alkylamines were treated with 2 equivalents of furfural, benzaldehyde, or paraformaldehyde, C-insertion of the carbonyl carbon occurred in the P-N bond with oxidation of phosphorus from P(III) to P(V). This is similar to the Pudovik reaction (Fig. 3.10a). The proposed mechanism for this reaction is illustrated in Figure 3.9. It begins with nucleophilic attack on the

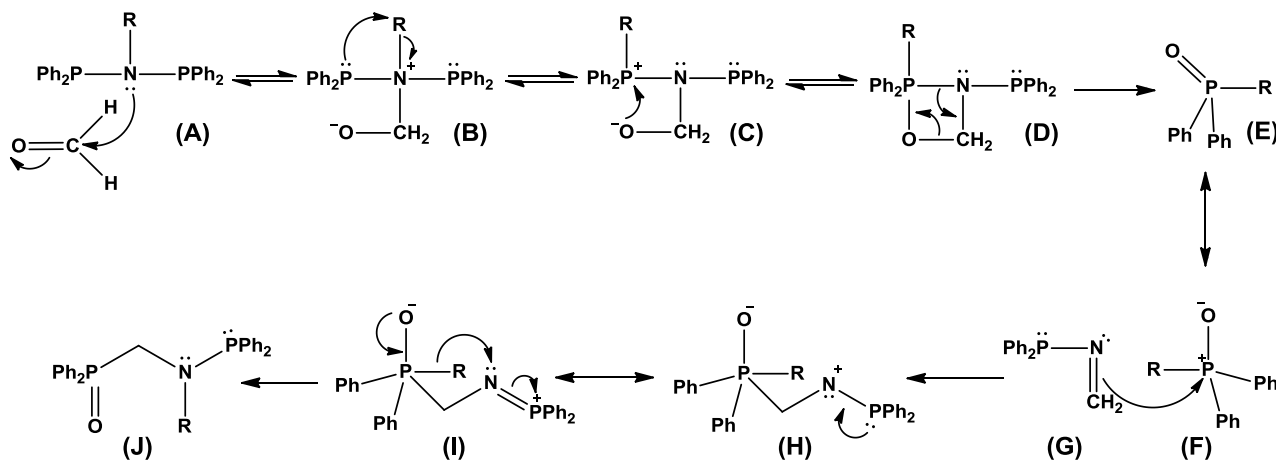


**Figure 3.9.** Proposed mechanism for C-insertion into a P-N bond.

carbonyl carbon by the nitrogen atom to form species **B**. The lone pair of electrons on the phosphorus atom attacks the R group on the positively charged ammonium ion, which forms species **C**. The negatively charged oxygen attacks the positive phosphorus center to form a

1,3,2-oxazaphosphorine compound (**D**). The oxazaphosphorine then forms a phosphine oxide (**E**) and an imine (**G**). Electrophilic addition of **F** onto the N-C double bond leads to the formation of complex **H** which has an electron deficient nitrogen. The positive charge on the nitrogen can be stabilized by the adjacent phosphorus atom (**I**) to allow migration of the R group and give the final product (**J**). Another possible reaction that can occur with aldehydes is the formation of  $\alpha$ -hydroxy phosphine oxides, similar to the Abramov reaction (Fig. 3.10b). This reaction occurs from an initial P-N bond cleavage to form  $\text{Ph}_2\text{P}(\text{O})\text{H}$ , which reacts with the aldehyde to form the  $\alpha$ -hydroxy phosphine oxide. These reactions (Fig. 3.8) have not yet been shown to occur while the ligand is bound to a metal center, which we find encouraging. But, if our catalyst does lose a rhodium center as proposed in Figure 3.2 structure **C**, formation of the  $\alpha$ -hydroxy phosphine oxide or C-insertion could occur when complex **C** is in solution with the aldehyde product of the hydroformylation reaction.

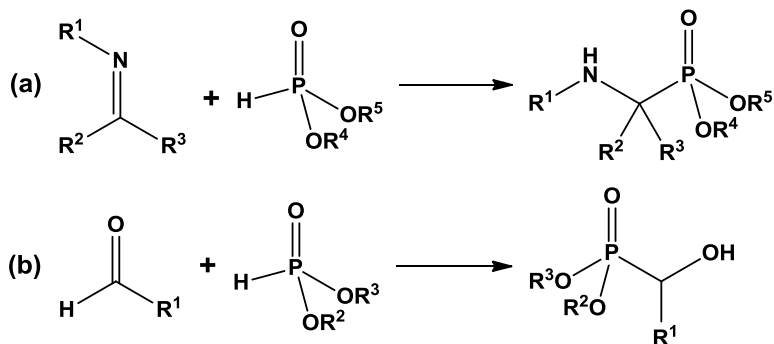


**Figure 3.10.** (a) Pudovik and (b) Abramov reactions.

### 3.5. Applications

After extensive searching, no literature results were obtained in which PNP ligands were used in hydroformylation catalysts. This is most likely due to the fact that the related PCP bridging or chelating ligands make poor hydroformylation catalysts. They are however used in several other reactions. In 1999, Gimbert and coworkers used a dicobalt compound containing a bridging PNP ligand with various substituents on the N and P atoms for use in asymmetric Pauson-Khand reactions.<sup>10</sup> These ligands were very effective in the reaction with yields >98%

with the bimetallic complex shown in Figure 3.11. These catalysts were also useful in providing the expected adduct from the less reactive indene in 72% yield, which is much higher than the best literature describing a 52% yield for this reaction.

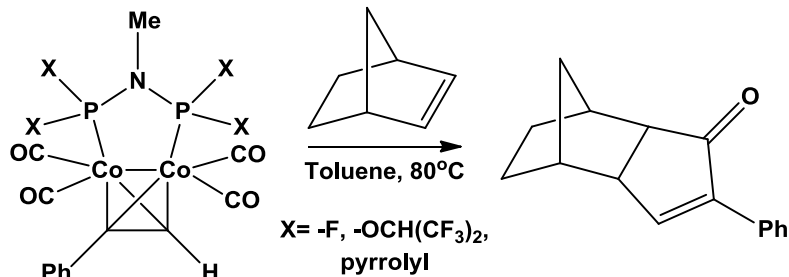


**Figure 3.11.** Bimetallic cobalt catalyst for asymmetric Pauson-Khand reactions.

These ligands have been utilized in polymerization/oligomerization catalysts. In 2001, Wass and coworkers reported a nickel (II) complex containing a bis(diarylphosphino)-methylamine ligand that was highly active toward the polymerization of ethylene yielding high molecular weight polymers (Fig. 3.12a).<sup>11</sup> Its performance was near that of the best nickel-based systems.<sup>12</sup> Another feature of this catalyst was that it was poison tolerant exhibiting activity with up to 10% (by volume) water content. In 2007, they also reported up to 95% isoprene trimerisation with PNP-chromium catalysts (Fig. 3.12b).<sup>13</sup> The activity, 660 h<sup>-1</sup>, was more than two orders of magnitude higher than all previously reported isoprene trimerisation catalysts.

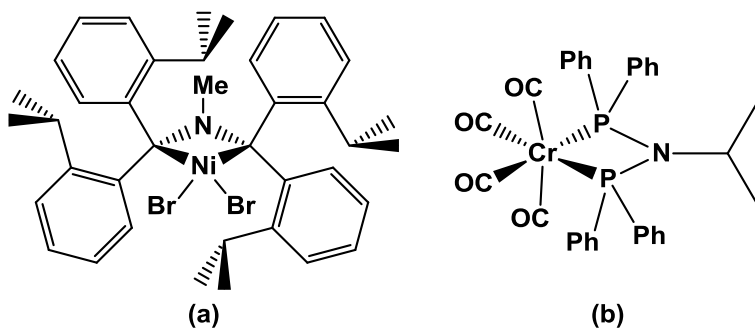


**Figure 3.12.** (a) Isoprene trimerisation catalyst; (b) Ethylene polymerization catalyst.

### 3.6. Retrosynthetic Analysis of the Aza-Bridged Ligand

To form the aza-bridged ligands, there are two possible disconnection points which would allow the ligand to be synthesized (Fig. 3.13). Most of the synthesis relies on the work performed by Monteil.<sup>1</sup> Monteil's work, based on that of Boymond *et al.*,<sup>14</sup> employed a simple iodine-magnesium exchange that was very effective in the synthesis of the arms of P4-Ph and

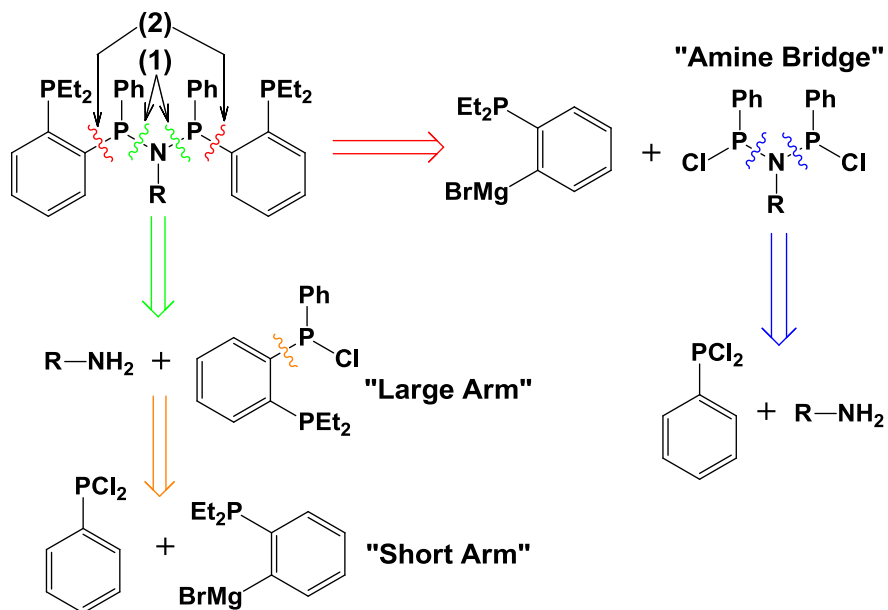


**Figure 3.13.** Retrosynthetic analysis of RN-P4-Ph ligands.

proceeded in greater than 90% yield. This technique was used to build both the "large arm" and "short arm." At disconnection 1, the large arm and a primary amine are coupled by an Sn<sub>2</sub> reaction to form the aza-bridged ligand. At disconnection 2, the short arm is coupled with an "amine bridge" through a Grignard-mediated reaction to form the aza-bridged ligand.

### 3.7. Synthesis of RN-P4-Ph by "Large Arm"-Amine Coupling

The short arm ((2-bromophenyl)diethylphosphine) is easily synthesized from 1-bromo-2-iodobenzene, isopropylmagnesium bromide, and diethylchlorophosphine in excellent yield (>85%) and is isolated by distillation under reduced pressure (Fig. 3.14a). To form the large arm (chloro(2-(diethylphosphino)phenyl)phenylphosphine), the same basic procedure is followed and dichlorophenylphosphine is reacted with the Grignard species (Fig. 3.14b). Attempts were

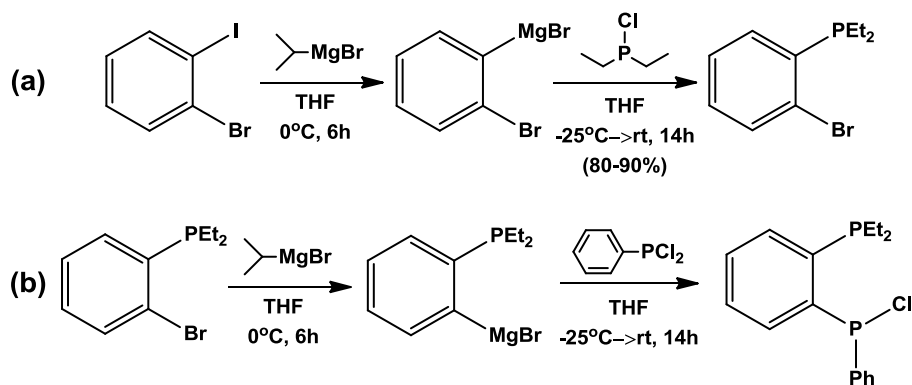


**Figure 3.14.** Preparation of (a) ((2-bromophenyl)diethylphosphine) and (b) chloro(2-(diethylphosphino)phenyl)phenylphosphine utilizing halide-magnesium exchange reactions.

made with several solvents (heptane, hexane, pentane, benzene, petroleum ether, dichloromethane, tetrahydrofuran) to isolate the desired large arm from the crude reaction mixture (white paste-like substance) but all were unsuccessful in giving a pure compound (Fig. 3.15). Distillation of the compound under an inert atmosphere at reduced pressure (0.25 Torr)

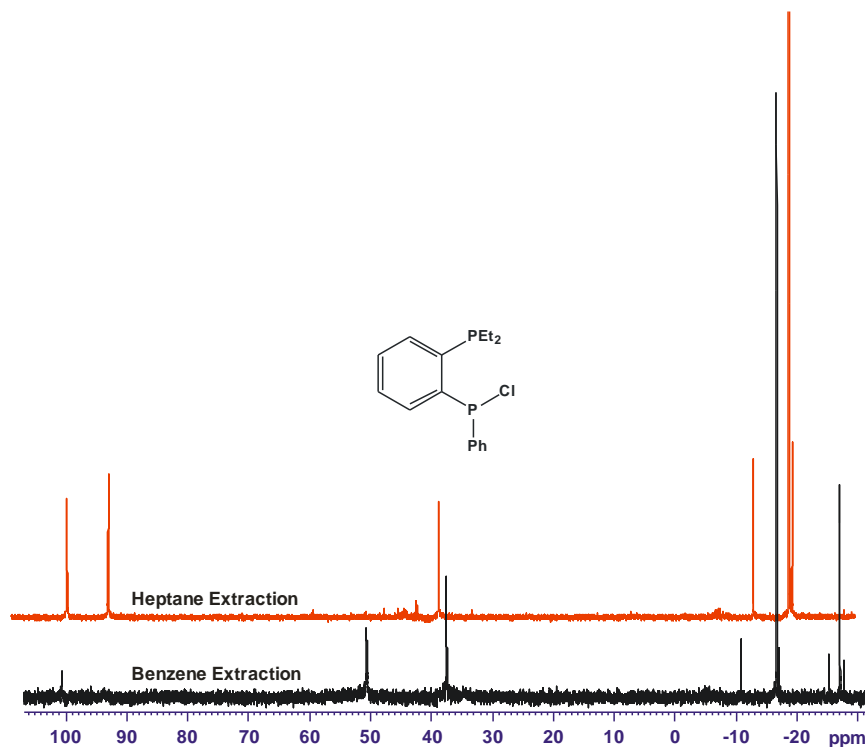


**Figure 3.15.**  $^{31}\text{P}$  NMR of heptane and benzene extraction of the large arm.

was unsuccessful and caused the product to decompose in the distilling flask due to the excessive heating (up to 280 °C). We believe that one way to combat the isolation problem is to



replace dichlorophenylphosphine with the mono protected species, (N,N-diethylamino)-chlorophenylphosphine. One problem faced when trying to extract the large arm is that it cannot be treated with water to remove magnesium salts and quench unreacted Grignard reagent due to the reactive halophosphine. Therefore, an organic solvent extraction is not very helpful. Prof. Stanley suggested quenching with an organic soluble anhydrous  $[\text{HNR}_3][\text{anion}]$  salt followed by an organic extraction. This has not been performed but is worth researching. If the large arm is made in which the P-Cl bond is replaced with P-NEt<sub>2</sub>, a successful extraction could possibly be performed and a pure compound isolated (Fig. 3.16). The protected phosphine is then treated

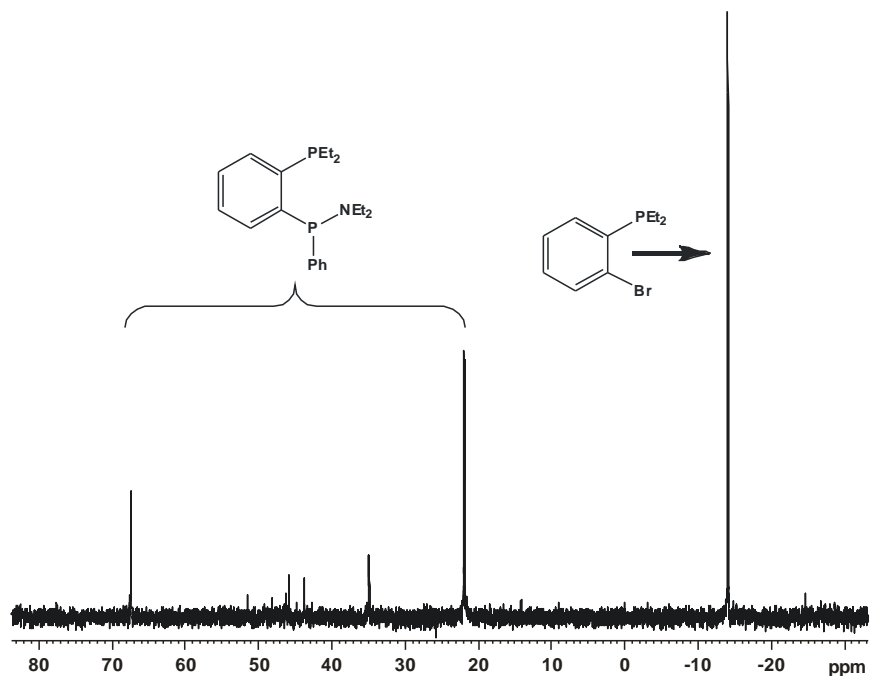


**Figure 3.16.**  $^{31}\text{P}\{^1\text{H}\}$  NMR of (N,N-diethylamino)[2(diethylphosphino)phenyl]phenylphosphine.

with 4 equivalents of ethereal HCl to obtain the large arm. Initial results seemed impressive for the synthesis of the mono-protected large arm. When the compound was deprotected with HCl, two products formed, a clear liquid and translucent crystals, both of which showed resonances in  $^{31}\text{P}\{^1\text{H}\}$  NMR (Fig. 3.17). The crystalline solid has been recrystallized by vapor diffusion crystallization and will soon be analyzed by x-ray crystallography. Prof. Stanley suggested that there is a possibility that the solid is the same species as the liquid product that has been

protonated by the large excess of HCl. This reaction needs to be performed again with a stoichiometric amount of ethereal HCl so that a protonated phosphorus species will be inhibited.

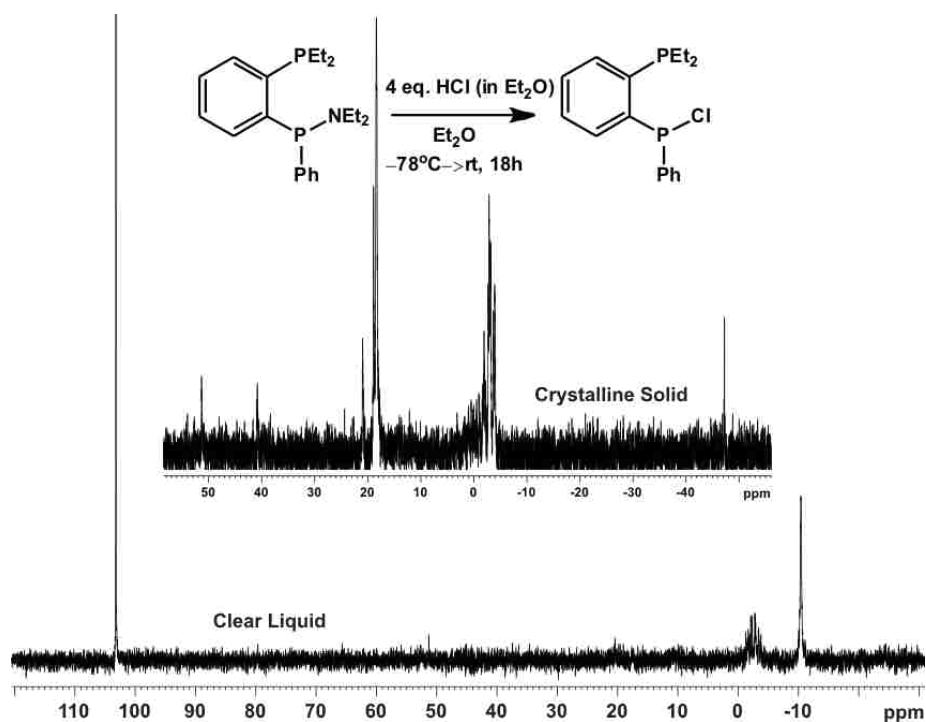


**Figure 3.17.**  $^{31}\text{P}\{^1\text{H}\}$  NMR spectra of products obtained from the deprotection of the mono-protected large arm.

The resonance at  $-14$  ppm in Figure 3.16 was thought to be the starting material, (2-bromophenyl)diethylphosphine, which failed to react with  $(i\text{Pr})\text{MgBr}$ . The Grignard reaction was performed a second time and it was confirmed by  $^{31}\text{P}\{^1\text{H}\}$  NMR that the reaction did go to completion. (N,N-diethylamino)chlorophenylphosphine was added dropwise at  $-25$  °C and the solution was stirred overnight. Upon quenching with water, a thick white precipitate formed in the aqueous layer. The organic layer was removed and the aqueous layer was extracted with diethyl ether. The  $^{31}\text{P}\{^1\text{H}\}$  NMR spectra (Fig. 3.18) of the crude organic extractions is somewhat different from the spectra obtained when it was first performed. The aqueous quench layer needs to be analyzed to determine what species makes up the white precipitate. This may give some insight on whether the peak at  $-14$  ppm is starting material that

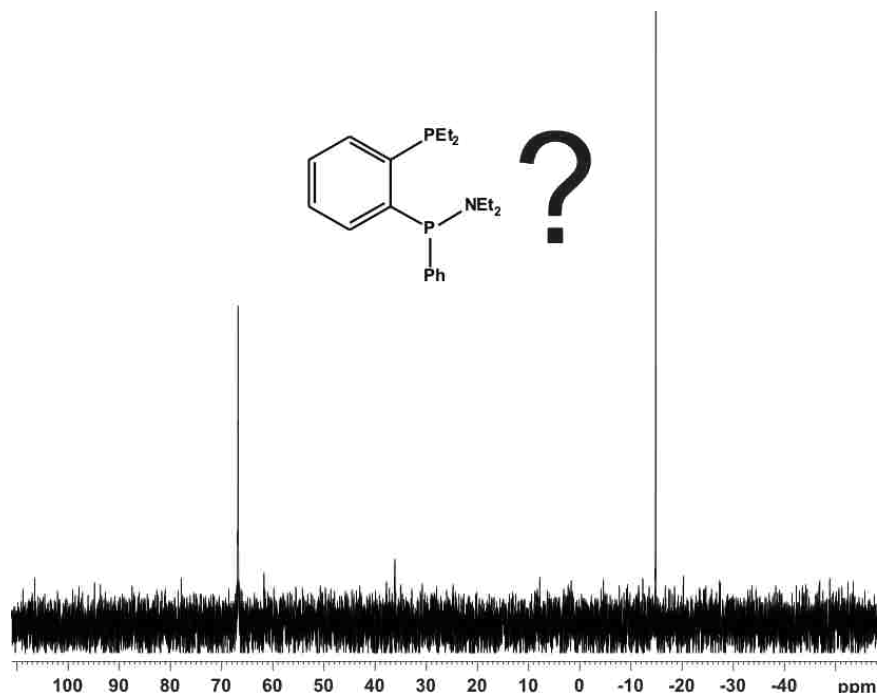


**Figure 3.18.**  $^{31}\text{P}\{^1\text{H}\}$  NMR of what might be (N,N-diethylamino)[2(diethylphosphino)phenyl]phenylphosphine from most recent synthesis.

reformed during the quench or if it is just a coincidence that the peak is the same as the starting material. Once this arm is obtained, coupling with a primary amine should afford the desired ligand, RN-P4-Ph.

### 3.8. Synthesis of RN-P4-Ph by Grignard-mediated “Small Arm”-Amine Bridge Coupling

The second synthetic approach to the aza-bridged ligands is using a Grignard-mediated coupling of the small arm and an amine bridge. The amine bridge is synthesized from a primary amine slowly treated with 2 equivalents of dichlorophenylphosphine at 0°C while trapping liberated HCl with excess pyridine or triethylamine (Fig. 3.19a). Filtration of the ammonium salts and removal of the solvent *in vacuo* affords the amine bridge in 30-40% yield. It was then discovered that the reaction to synthesize the amine-bridges never went to completion. Some dichlorophenylphosphine was always present in the final solution. To correct this, the final mixture was treated again with 1 equivalent of the primary amine and excess pyridine or triethylamine. This additional reaction was used to recently synthesize the tert-butyl amine

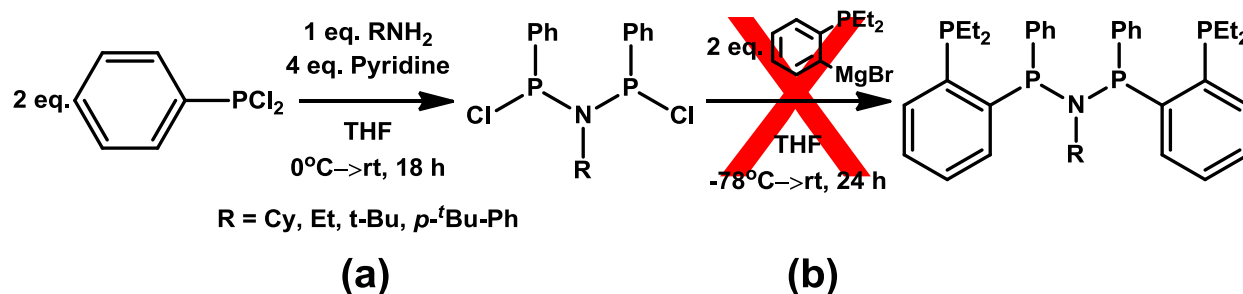


**Figure 3.19.** Synthetic scheme involving a Grignard-mediated coupling.

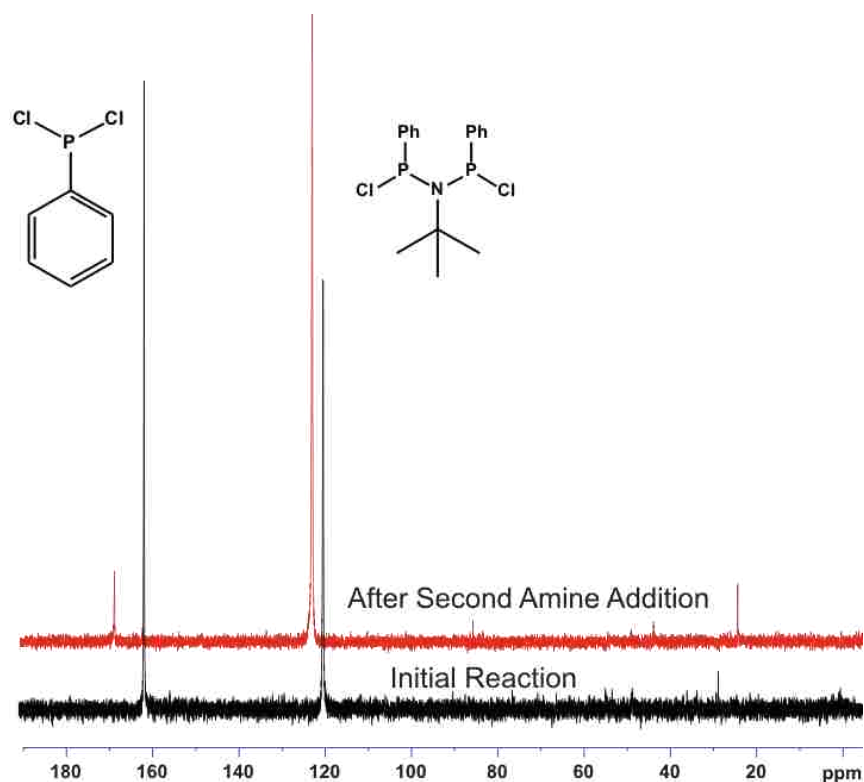


**Figure 3.20.**  $^{31}\text{P}\{^1\text{H}\}$  NMR of t-butyl amine bridge after the initial reaction and second amine addition.

bridge and Figure 3.20 shows a large increase in the product peak (~120 ppm) and a large decrease in the size of the dichlorophenylphosphine peak (~162 ppm). The ethyl and cyclohexyl amine bridges need to be resynthesized according to this procedure in order to obtain pure compounds. The most recent amine bridge to be attempted is *para*-tert-butyl aniline as the primary amine used. The crude  $^{31}\text{P}\{^1\text{H}\}$  NMR for this bridge (Fig. 3.21) shows two possible product peaks (112 ppm, 126 ppm) and a dichlorophenylphosphine peak (~162 ppm). An

attempt to remove the dichlorophenylphosphine by vacuum distillation (heated only to 85 °C to prevent decomposition) was made but without success. However, all the peaks in the NMR spectra changed. There was a decrease in the dichlorophenylphosphine peak, an increase of the peak at 126 ppm, and a decrease in the peak at 112 ppm. It is possible that the reaction

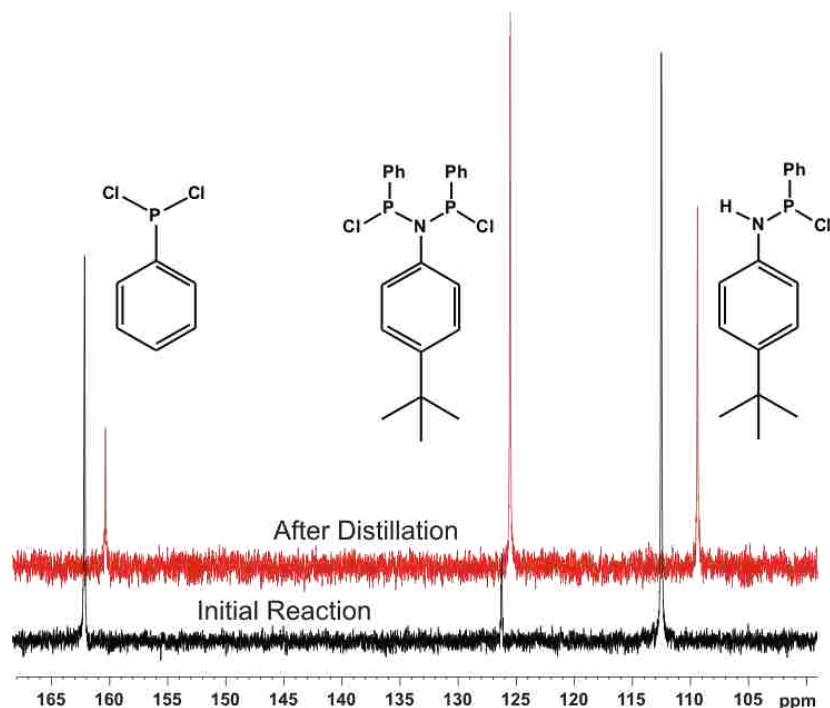


**Figure 3.21.**  $^{31}\text{P}\{^1\text{H}\}$  NMR of the initial reaction to form p-tert-butyl aniline bridge and after distillation.

requires more vigorous conditions to go to completion and that the peak at 112 ppm is the intermediate compound to the amine bridge.

The coupling step (Fig. 3.19b) was attempted between the cyclohexyl and tert-butyl amine bridges (both not purified) and the short arm but was unsuccessful after stirring at room temperature for 24 hours. The crude reaction mixture contained only the initial reactants when analyzed by  $^{31}\text{P}\{^1\text{H}\}$  NMR. Refluxing the mixture for an additional 24 hours was attempted in hopes that more vigorous reaction conditions would cause the desired reaction to occur but with no success.

P(III)-N bonds are displayed as single bonds but analyzing bond length shows that there is some double bond character present. A P-N single bond is approximately 1.75 Å – 1.80 Å, whereas the P-N bond lengths in PNP ligands are approximately 1.60 Å – 1.69 Å. Partial double bond character most likely occurs because of the  $\pi$ -interaction between the  $p$  orbital of the nitrogen and an empty  $d$  orbital of each of the phosphorus atoms. Furthermore, the decrease in reactivity of the phosphorus atoms on the bridge is due to the nitrogen center. The lone pair on the nitrogen atom increases the nucleophilicity of the phosphorus atoms. Normally, the phosphorus can act as an electrophile in a substitution reaction because of the empty  $d$  orbitals, but an increase in nucleophilicity will make the phosphorus less susceptible to nucleophilic attack.

The Finkelstein reaction is a reaction in which an alkyl chloride or alkyl bromide is treated with sodium iodide (or potassium iodide) in acetone to afford an alkyl iodide.<sup>3,15</sup> The transformation can occur by an  $S_N1$  or  $S_N2$  reaction depending on the nature of the alkyl halide. This reaction is an equilibrium reaction that follows Le Chatelier's principle. Sodium iodide is much more soluble in acetone than sodium chloride and bromide and the precipitation of these salts drives the reaction to completion by removing the chloride and bromide ions from solution.

This same methodology was applied to the amine bridge in hopes that the phosphorus centers would be more reactive to nucleophilic attack with replacement of the chlorines for the better leaving group, iodine. The amine bridge was allowed to stir in the presence of KI for 24 hours in THF (Fig. 3.22a). As time progressed, the solution became more orange and a yellow precipitate formed, which is indicative of the less soluble KCl. The reaction was monitored by  $^{31}\text{P}\{^1\text{H}\}$  NMR, but due to poor spectra, the proof of a halide exchange is not definitive. The last coupling step (Fig. 3.22b) has been performed without purification of the iodine-containing bridge and isolation of the product has been attempted. The product that was formed was more soluble in the aqueous layer than the organic layer and remained in the aqueous layer after

workup. This was not observed until the aqueous layer was neutralized with bleach before discarding. This sequence of reactions needs to be performed again and careful isolation of each intermediate must be done in order to obtain clear evidence that the desired products are being made. Also, the amine bridge was thought to be pure when the initial Finkelstein-type reaction was performed, however there was unreacted dichlorophenylphosphine present from the synthesis of the bridge.

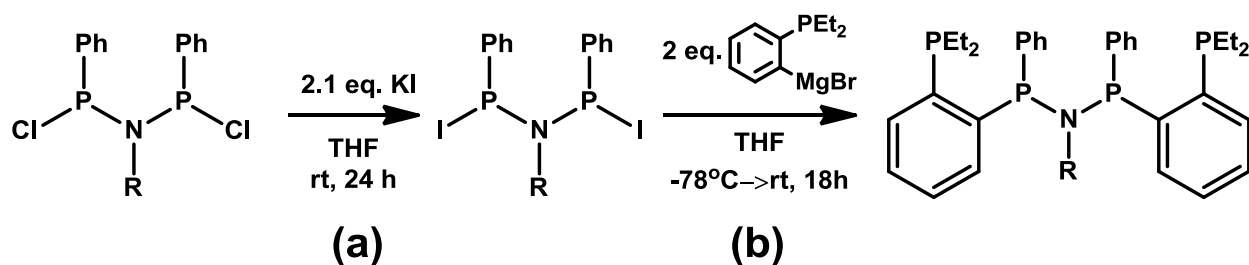


**Figure 3.22.** Synthesis of RN-P4-Ph utilizing the Finkelstein reaction.

### 3.9. Future Work

Our work has not yet afforded us with the RN-P4-Ph ligands, which is our main focus at this point. Synthesis of the large arm through the protected derivative followed by coupling with the primary amine will be attempted. The Finkelstein-type reaction to give us the desired ligand has been completed, but the ligand has not yet been isolated. If one of these paths is successful, separation of the isomers is the next challenge. Solvent crystallization will be attempted first since it gives a good separation of the et,ph-P4 ligand. Separation of the isomers may be possible by HPLC, which should also be attempted.

To date, no considerable effort has been made to achieve a resolution of the ligand isomers with chiral resolving agents. Diastereomeric crystallization of chiral molecules by way of chiral resolving agents is an older, well known method to obtain the desired compound. This process is performed by a trial-and-error basis due to the large number of resolving agents and solvent variations. The most likely chiral compounds to give the desired separation are

carboxylic acids, such as amino acids, tartaric acids, etc.. I believe that this would be a good project to invest time into as it might prove very beneficial to our ligand separation problems.

### 3.10. References

1. Monteil, A. R. Ph. D. Dissertation, Louisiana State University, Baton Rouge, LA, 2006.
2. Leeuwen, P. W. N. M. v.; Claver, C. *Rhodium Catalyzed Hydroformylation*; Kluwer Academic Publishers: Dordrecht [Netherlands]; Boston, 2000.
3. Matthews, R. C.; Howell, D. K.; Peng, W. J.; Train, S. G.; Treleaven, D. W.; Stanley, G. G. *Angew. Chem. Int. Ed.*, **1996**, *35*, 2253.
4. Browning, C. S.; Farrar, D. H.; Peterson, M. R. *J. Mol. Structure (Theochem)* **1991**, *251*, 153.
5. Prabusankar, G.; Palanisami, N.; Murugavel, R.; Butcher, R. J. *Dalton Trans.* **2006**, 2140.
6. Hill, T. G.; Haltiwanger, R. C; Prout, T. R; Norman, A. D. *Inorg. Chem.* **1989**, *28*, 3461.
7. Balakrishna, M. S.; Reddy, V. S.; Krishnamurthy, S. S.; Nixon, J. F.; St. Laurent, J. C. T. R. B. *Coord. Chem. Rev.* **1994**, *129*, 1.
8. (a) Newton, M. G.; King, R. B.; Chang, M.; Gimeno, J. *J. Am. Chem. Soc.* **1978**, *100*, 5. (b) King, R. B.; Gimeno, J. *J. Chem. Soc., Chem. Commun.* **1977**, 142. (c) Newton, M. G.; King, R. B.; Chang, M.; Gimeno, J. *J. Am. Chem. Soc.* **1977**, *99*, 2802. (d) Newton, M. G.; King, R. B.; Chang, M.; Pantaleo, N. S.; Gimeno, J. *J. Chem. Soc., Chem. Commun.* **1977**, 531. (f) King, R. B.; Chen, K.-N. *Inorg. Chim. Acta.* **1977**, *L19*, 23.
9. (a) Priya, S.; Balakrishna, M. S.; Mague, J. T.; Mobin, S. M. *Inorg. Chem.* **2003**, *42*, 1272. (b) Priya, S.; Balakrishna, M. S.; Mague, J. T. *Inorg. Chem. Comm.* **2001**, *4*, 437.
10. Gimbert, Y.; Robert, F.; Durif, A.; Averbuch, M. T.; Kann, N.; Greene, A. E., *J. Org. Chem.* **1999**, *64*, 3492.
11. Heslop, K.; Orpen, A. G.; Pringle, P. G.; Cooley, N. A.; Green, S. M.; Wass, D. F. *Organometallics* **2001**, *20*, 4769.
12. (a) Johnson, L. K.; Killian, C. M.; Brookhart, M. *J. Am. Chem. Soc.* **1995**, *117*, 6414. (b) Younkin, T. R.; Connor, E. F.; Henderson, J. I.; Friedrich, S. K.; Grubbs, R. H.; Bansleben, D. A. *Science* **2000**, *287*, 460. (c) Gates, D. P.; Svejda, S. A.; Onate, E.; Killian, C. M.; Johnson, L. K.; White, P. S.; Brookhart, M. *Macromolecules* **2000**, *33*, 2320.
13. Bowen, L. E.; Charernsuk, M.; Wass, D. F., *Chem. Comm.* **2007**, 2835.
14. Boymond, L.; Rottlander, M.; Cahiez, G.; Knochel, P. *Angew. Chem. Int. Ed.* **1998**, *37*, 1701.



## Chapter 4: Experimental Section

All synthetic procedures were performed using standard Schlenk and dry box techniques. All solvents and chemicals used were purchased from Aldrich and used without further purification.  $^{31}\text{P}$  NMR spectra were recorded on a Bruker 250 MHz spectrometer. Chemical shifts are reported relative to  $\text{H}_3\text{PO}_4$  (external standard).

### 4.1. Synthesis of (2-Bromophenyl)diethylphosphine

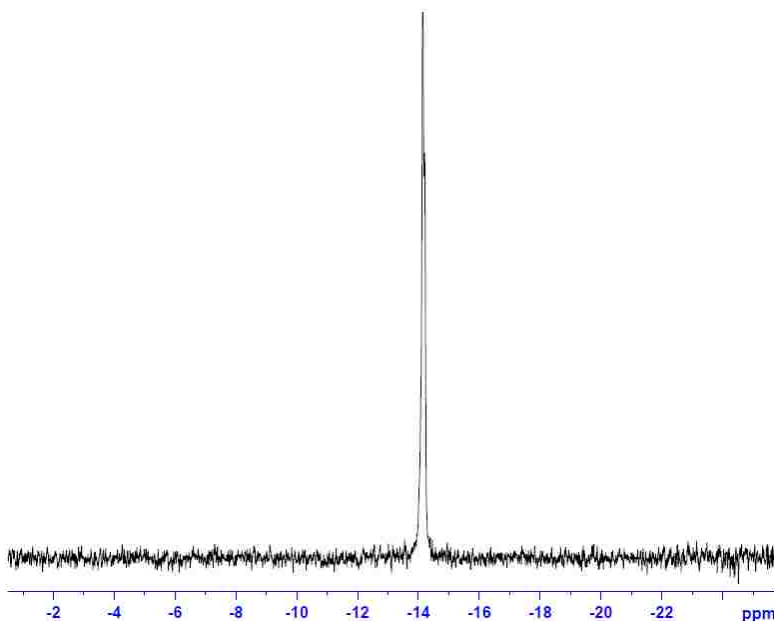


**Figure 4.1.**  $^{31}\text{P}\{^1\text{H}\}$  NMR of (2-bromophenyl)diethylphosphine.

A solution of 1-bromo-2-iodobenzene (60.45 g, 214 mmol) in THF (200 mL) is treated at 0 °C with a 1.089 M solution of isopropylmagnesium bromide in THF (203 mL, 221 mmol) which is diluted with THF (200 mL). The Grignard solution is kept at 55 °C to prevent the cannula from becoming clogged. The resulting solution is stirred at 0 °C for 6 h. The solution, remaining at 0 °C, is added dropwise to diethylchlorophosphine (26.61 g, 214 mmol) in THF (200 mL), which is cooled to -25 °C. The slightly yellow solution is allowed to warm to room temperature and stir overnight. Water (100 mL) is added, and the organic layer is separated. The aqueous layer is extracted with diethyl ether (3 x 100 mL). The organic extracts are combined and dried over

Na<sub>2</sub>SO<sub>4</sub>. All solvent is removed *in vacuo* to yield a slightly yellow liquid. The product is distilled *via* short-path distillation *in vacuo* to yield 37.18 g (152 mmol) of an air/light-sensitive, colorless liquid: bp 116-122 °C (0.25 Torr).

% Yield: 71%

<sup>31</sup>P{<sup>1</sup>H} NMR (C<sub>6</sub>D<sub>6</sub>): δ = -14.1 (s)

#### 4.2. Synthesis of Chloro(N,N-diethylamino)phenylphosphine

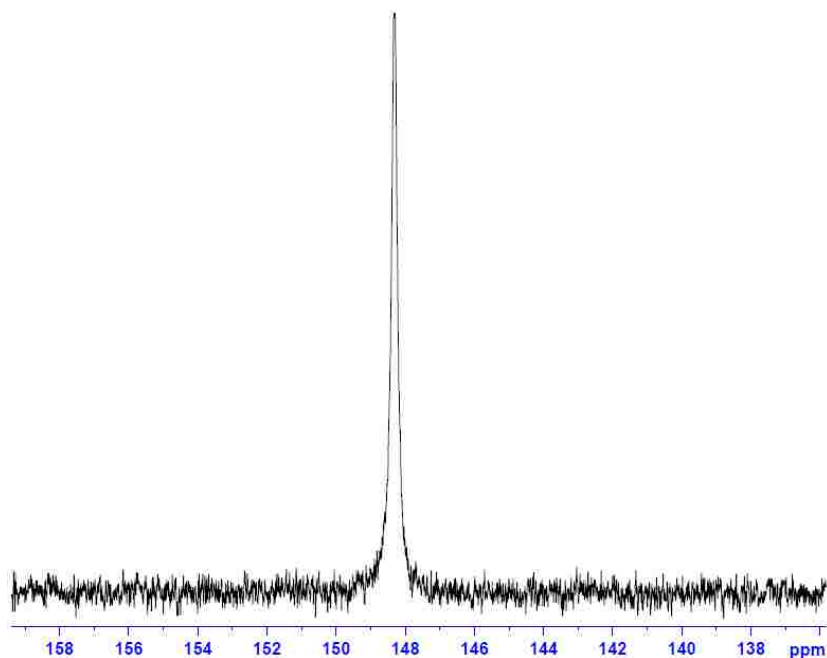


**Figure 4.2.** <sup>31</sup>P{<sup>1</sup>H} NMR of chloro(N,N-diethylamino)phenylphosphine.

A solution of dichlorophenylphosphine (50.00 g, 279 mmol) in petroleum ether (400 mL) is cooled to -78 °C. Diethylamine, 2.5 equivalents, (51.08 g, 698 mmol) in petroleum ether (50 mL) is added dropwise (rate: 1 drop/s) to the phosphine. Upon completion, the solution is allowed to slowly warm to room temperature while stirring overnight to result in a light yellow liquid with a white precipitate. The solution is filtered in the glovebox through a coarse fritted funnel to remove all ammonium salts, and the white precipitate is rinsed several times with petroleum ether. The solvent is removed *in vacuo* to yield a non-viscous, cloudy, light yellow liquid (36.72 g, 170 mmol). The product is distilled *in vacuo* with a Vigreux column to separate

the desired product from the starting material, collecting the fraction between 65-90 °C (0.25 Torr).

% Yield: 61%

$^{31}\text{P}\{^1\text{H}\}$  NMR ( $\text{C}_6\text{D}_6$ ):  $\delta = 148.3$  (s)

#### 4.3. Attempted Synthesis of (N,N-diethylamino)(2-(diethylphosphino)phenyl)-phenylphosphine

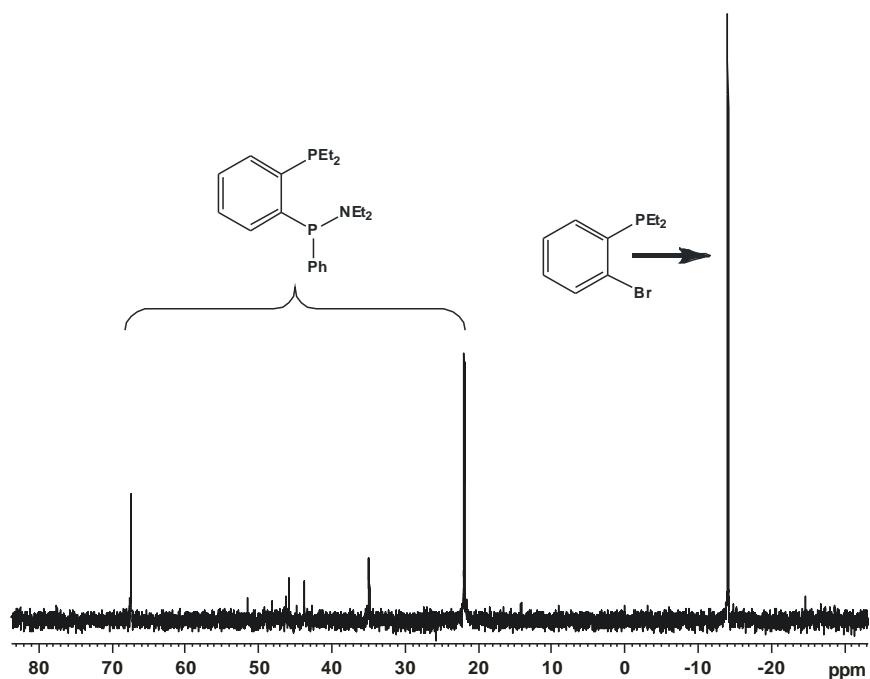


**Figure 4.3.**  $^{31}\text{P}\{^1\text{H}\}$  NMR of (N,N-diethylamino)(2-(diethylphosphino)phenyl)phenylphosphine.

A solution of (2-bromophenyl)diethylphosphine (5.87 g, 24.0 mmol) in THF (80 mL) is cooled to 0 °C. A 0.665 M solution of isopropylmagnesium bromide in THF (at 50 °C) is added to the previous solution dropwise via cannula. The resulting solution is stirred at 0 °C for 6 h. After 6 h, it is added dropwise via cannula, while still at 0 °C, to a solution of chloro(N,N-diethylamino)phenylphosphine (5.23 g, 24.3 mmol) in THF (50 mL) which was cooled to -78 °C. The resulting solution is allowed to slowly warm to room temperature while stirring overnight to yield a transparent, orange solution. Water (18 mL) is added and the organic layer is separated.

The aqueous layer is extracted with diethyl ether (3 x 50 mL). The organic extracts are combined and dried over Na<sub>2</sub>SO<sub>4</sub>. It is filtered and the solvent is removed *in vacuo*. Product was carried to the next step (reacted with ethereal HCl; yield was calculated to be greater than 100% so it was reacted with HCl assuming it was 100%).

% Yield: 108% (may be due to residual amine)

<sup>31</sup>P{<sup>1</sup>H} NMR (C<sub>6</sub>D<sub>6</sub>): δ = 67.4 ppm (s), 51.5 ppm (s), 48.2 ppm (s), 46.3 ppm (s), 45.8 ppm (s), 43.7 ppm (s), 34.9 ppm (s), 21.9 ppm (s), -14.1 (s)

#### 4.4. Attempted Synthesis of Chloro(2-(diethylphosphino)phenyl)phenylphosphine

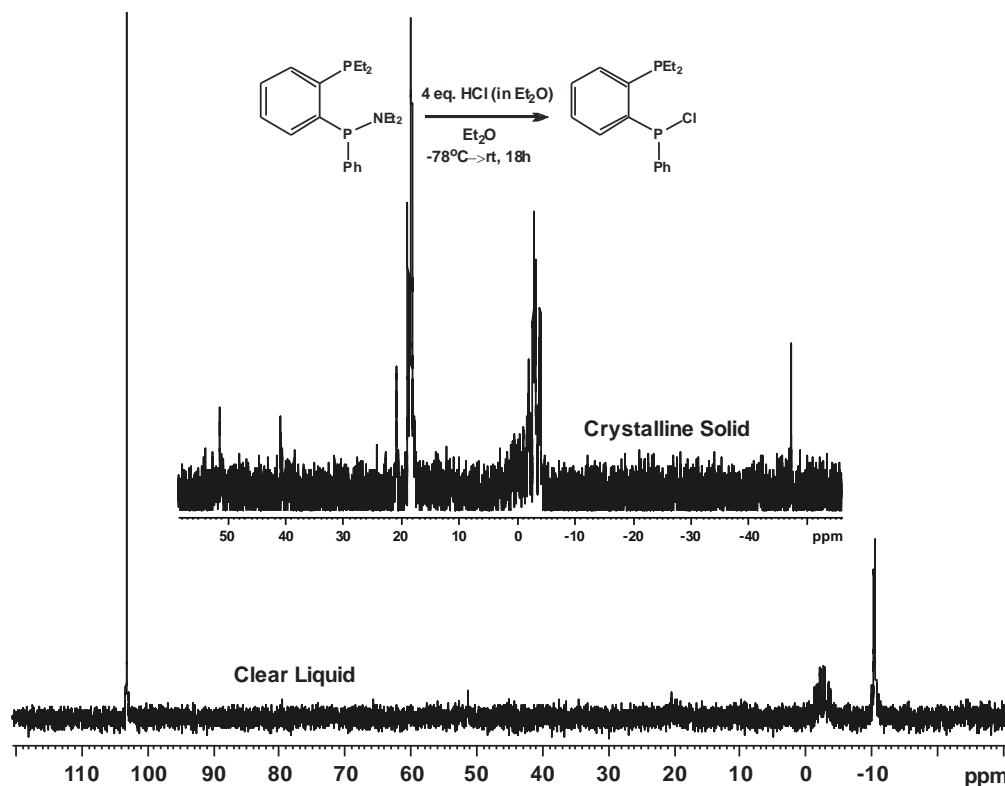


**Figure 4.4.** <sup>31</sup>P{<sup>1</sup>H} NMR of the products obtained in the synthesis of chloro(2-(diethylphosphino)phenyl)phenylphosphine.

A solution of 2 M ethereal HCl (52 mL, 104 mmol) is treated dropwise at -78 °C with a solution of (N,N-diethylamino)(2-(diethylphosphino)phenyl)phenylphosphine (8.948 g, 25.9 mmol) in diethyl ether (38 mL). Once the addition is complete, the solution is allowed to warm to room

temperature and stir overnight. The solvent was removed *in vacuo* to result in a viscous liquid and a clear, crystalline precipitate.

% Yield: Not calculated due to the formation of a liquid and a solid product

$^{31}\text{P}\{^1\text{H}\}$  NMR ( $\text{C}_6\text{D}_6$ ): FOR SOLID PRODUCT:  $\delta = 51.3$  ppm (s), 40.8 ppm (s), 21.0 ppm (s), 18.9 and 18.4 ppm (d),  $-1.9$  ppm (t),  $-3.1$  ppm (t),  $-3.7$  and  $-3.9$  ppm (d),  $-47.2$  ppm (s)

FOR LIQUID PRODUCT:  $\delta = 103.2$  ppm (s),  $-2.1$  -  $-2.9$  (m),  $-10.4$  ppm (s)

#### 4.5. Attempted Synthesis of Bis(chlorophenylphosphino)cyclohexylamine

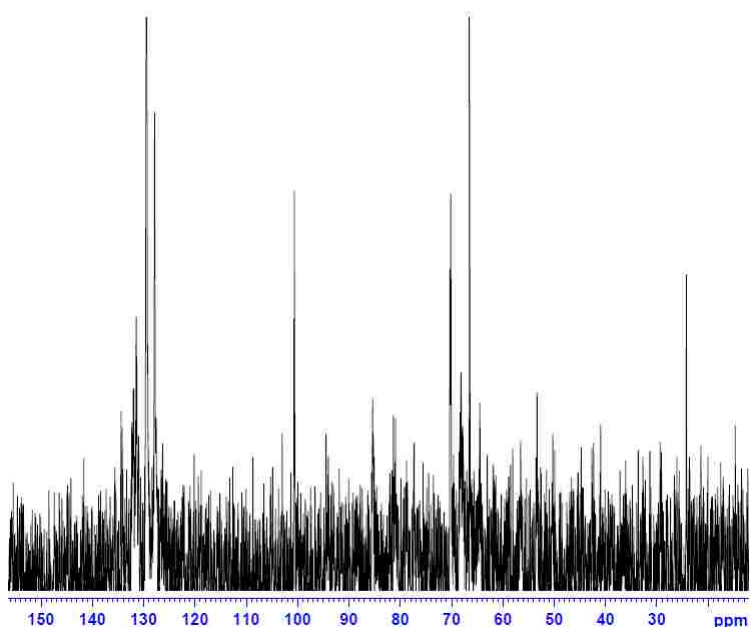


**Figure 4.5.**  $^{31}\text{P}\{^1\text{H}\}$  NMR of bis(chlorophenylphosphino)cyclohexylamine.

A solution of dichlorophenylphosphine (17.906 g, 100 mmol) in THF (65 mL) is treated with cyclohexylamine (4.966 g, 50.1 mmol) and excess pyridine (16.201 g, 206 mmol) in THF (80 mL) at 0 °C. The resulting yellow solution was allowed to warm to room temperature and stir overnight. A precipitate formed and half of the solvent was removed *in vacuo*. The solution was cooled to near freezing, filtered through a coarse fritted funnel, and the solids in the funnel were rinsed with cold THF. The filtrate and rinses were combined and passed through a neutral alumina column and rinsed with THF. The solvent was removed *in vacuo* to result in 13.837 g

(36 mmol) of a light yellow oil. The percent yield was not accurate because the product was not purified.

$^{31}\text{P}\{^1\text{H}\}$  NMR ( $\text{C}_6\text{D}_6$ ): 129.5 ppm (s), 127.9 ppm (s) (all other peaks are impurities)

#### 4.6. Attempted Synthesis of Bis(chlorophenylphosphino)ethylamine

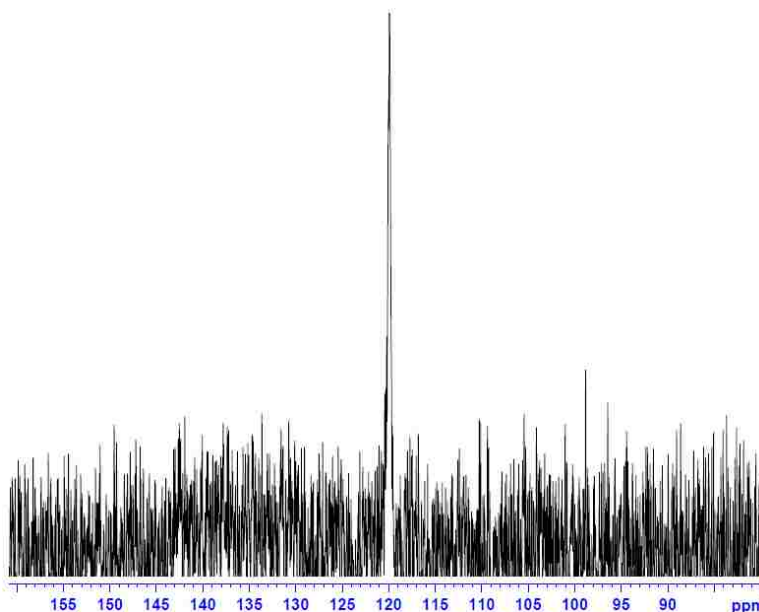


**Figure 4.6.**  $^{31}\text{P}\{^1\text{H}\}$  NMR of bis(chlorophenylphosphino)ethylamine.

A 50 mmol batch was used. The product (10.674g, 32 mmol) was a translucent orange oil. The percent yield was not accurate because some dichlorophenylphosphine was still present.

$^{31}\text{P}\{^1\text{H}\}$  NMR ( $\text{C}_6\text{D}_6$ ): 135.6 ppm (s)

#### 4.7. Attempted Synthesis of Bis(chlorophenylphosphino)butylamine

A 50 mmol batch was used. The product (6.805 g, 19 mmol) was a translucent orange oil which contained dichlorophenylphosphine. It was then diluted with 75 mL THF and one equivalent of tert-butylamine and 4 equivalents pyridine were added slowly at 0 °C. The solution was stirred for 4 h at room temperature, the ammonium salts were filtered and rinsed with cold THF, and the solvent was removed in vacuo. The percent yield was not calculated as a small amount of dichlorophenylphosphine was still present.

$^{31}\text{P}\{^1\text{H}\}$  NMR ( $\text{C}_6\text{D}_6$ ): 119.9 ppm (s), 162 ppm (s) (dichlorophenylphosphine)

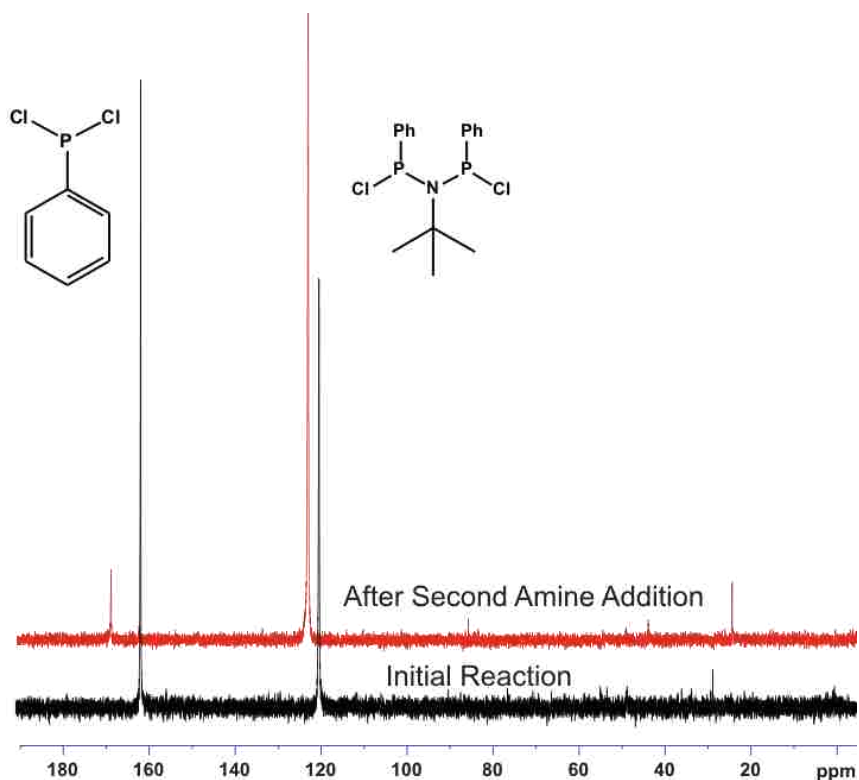


**Figure 4.7.**  $^{31}\text{P}\{^1\text{H}\}$  NMR of bis(chlorophenylphosphino)t-butylamine.

#### 4.8. Attempted Synthesis of Bis(chlorophenylphosphino)*p*-t-butylaniline

A solution of para-tert-butylaniline (3.733 g, 25 mmol) and pyridine (7.92 g, 100 mmol) in 100 mL THF were added dropwise at 0 °C to a solution of dichlorophenylphosphine (8.995 g, 50 mmol) in 50 mL THF. Upon completion of the addition, it was allowed to stir for 4 h at room temperature. Approximately half of the solvent was removed *in vacuo* and the solution was filtered while cooled to near freezing and the ammonium salts were rinsed with near freezing THF. The crude  $^{31}\text{P}\{^1\text{H}\}$  NMR showed presence of dichlorophenylphosphine so the product mixture was attempted to be distilled *in vacuo* up to 85 °C but no dichlorophenylphosphine came over in the receiving flask. Another NMR was taken in which the peaks changed as follows: 162 ppm (dichlorophenylphosphine) decreased, 126 ppm increased, and 112 ppm

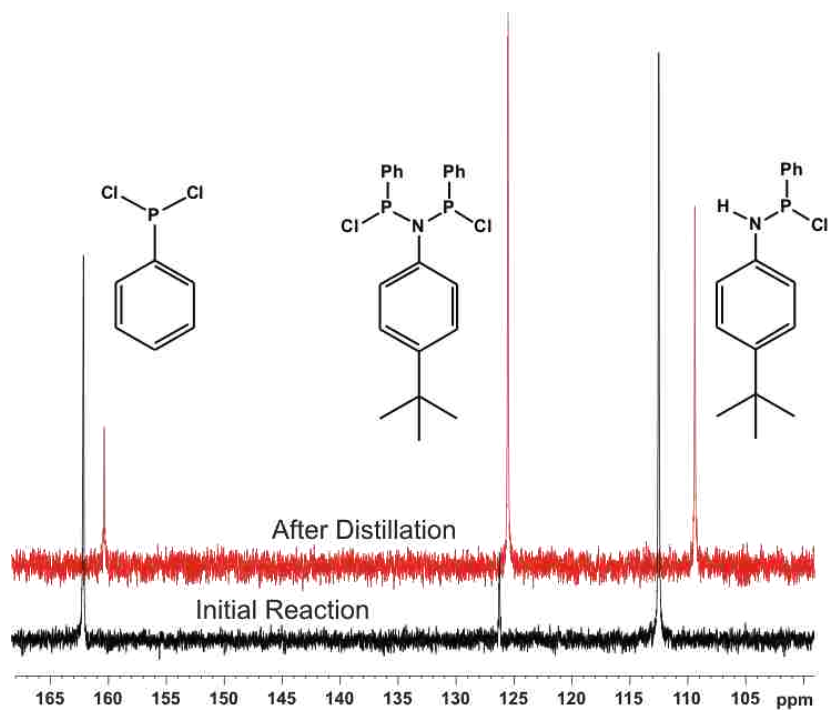


**Figure 4.8.**  $^{31}\text{P}\{^1\text{H}\}$  NMR of bis(chlorophenylphosphino)*p*-*t*butylaniline.

been calculated since a pure product has not been isolated.

$^{31}\text{P}\{^1\text{H}\}$  NMR ( $\text{C}_6\text{D}_6$ ): 112 ppm (s), 126 ppm (s), 162 ppm (s) (dichlorophenylphosphine)

#### 4.9. Synthesis of Phenylphosphine

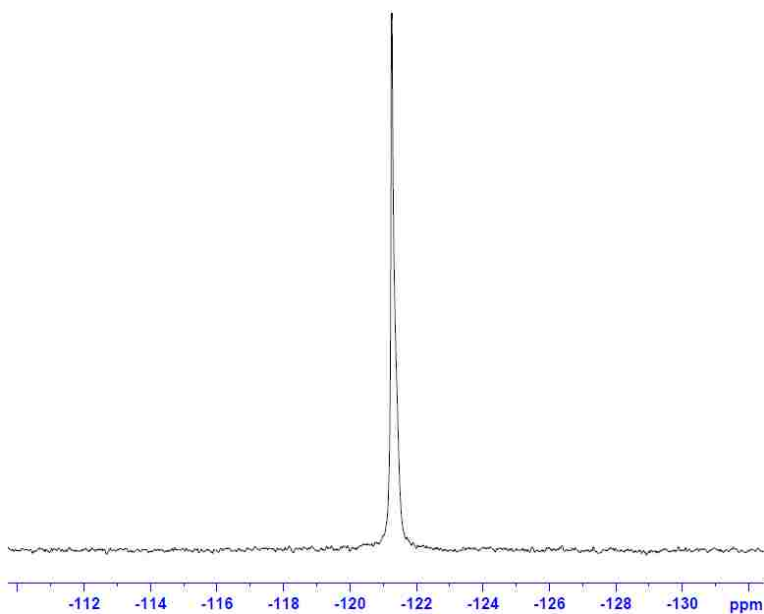


**Figure 4.9.**  $^{31}\text{P}\{^1\text{H}\}$  NMR of phenylphosphine.



A solution of dichlorophenylphosphine (37.5 g, 203 mmol) in t-glyme (160 mL) is slowly treated with lithium aluminum hydride (10.0 g, 256 mmol) in t-glyme (285 mL) while both are at 0 °C. The solution is allowed to warm to room temperature and stir overnight. The product is isolated via trap-to-trap distillation as a clear, colorless liquid (18.979 g, 172 mmol).

Yield: 79%

$^{31}\text{P}\{^1\text{H}\}$  NMR ( $\text{C}_6\text{D}_6$ ):  $\delta = -121$  ppm (s)

#### 4.10. Synthesis of Bis(phenylphosphino)methane

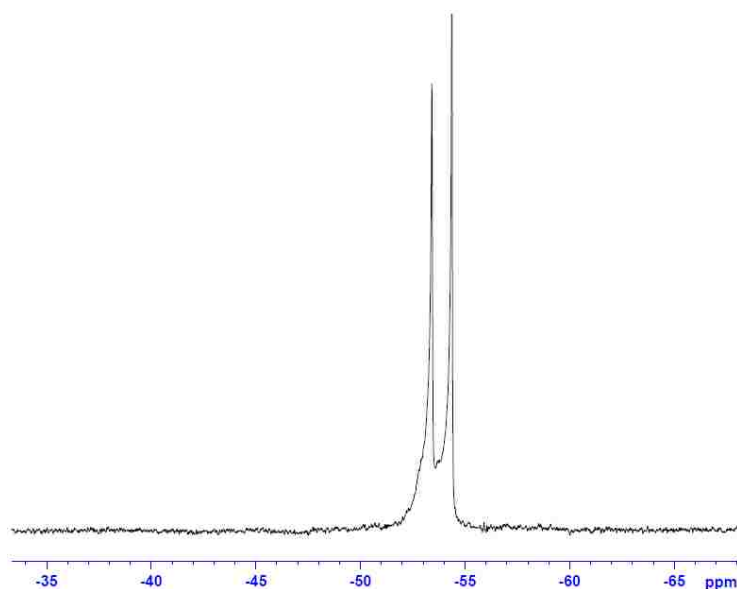


**Figure 4.10.**  $^{31}\text{P}\{^1\text{H}\}$  NMR of bis(phenylphosphino)methane.

A solution of phenylphosphine (17.6 g, 160 mmol), dichloromethane (6.9 g, 81 mmol), in N,N-dimethylformamide (150 mL) is slowly treated with 58% v/v aqueous potassium hydroxide (32 g, 570 mmol) while both are at 0 °C. This resulted in the formation of a yellow precipitate and orange solution. The solution was slowly warmed to room temperature and stirred overnight which resulted in white precipitate and a clear, colorless solution. Degassed water (50 mL) was added and the precipitate dissolved within 30 minutes. The aqueous layer was extracted with pentane (3 x 65 mL) and dried over anhydrous sodium sulfate. The solvent was removed *in vacuo* to yield a clear, colorless liquid (8.096g, 35 mmol).

Yield: 44%

$^{31}\text{P}\{^1\text{H}\}$  NMR ( $\text{C}_6\text{D}_6$ ):  $\delta = -53$  ppm (s) (racemic),  $-54$  ppm (s) (meso)

#### 4.11. Synthesis of Diethylchlorophosphine

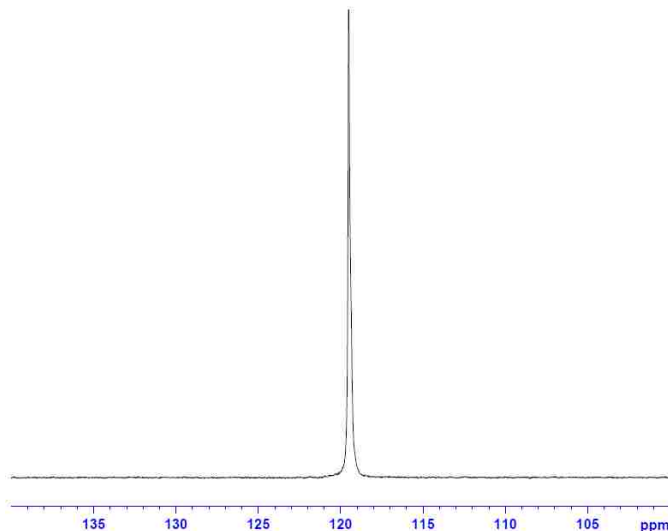


**Figure 4.11.**  $^{31}\text{P}\{^1\text{H}\}$  NMR of diethylchlorophosphine.

A solution of phosphorus trichloride (70.90 g, 515 mmol) in t-glyme (90 mL) is slowly treated with a 10% excess of diethylzinc (70.12 g, 567 mmol) in t-glyme (120 mL) while both solutions are kept at 0 °C. The solution is allowed to warm to room temperature and stir for 1 hour. The product, a clear, colorless liquid, is isolated by trap-to-trap distillation (53.39 g, 429 mmol).

Yield: 83%

$^{31}\text{P}\{^1\text{H}\}$  NMR ( $\text{C}_6\text{D}_6$ ):  $\delta = -128$  ppm (s)

#### 4.12. Synthesis of Vinyl-diethylphosphine

A solution of vinyl magnesium bromide (111 mL (1 M in THF), 111 mmol; 20% excess) and t-glyme (100 mL) is heated in vacuo to remove all THF. It is then slowly treated with diethylchlorophosphine (11.4 g, 91.5 mmol) in t-glyme (100 mL) while a temperature of 0 °C is maintained. Trap-to-trap distillation affords the clear, colorless liquid product (8.26 g, 71.1 mmol).

Yield: 78%

$^{31}\text{P}\{^1\text{H}\}$  NMR ( $\text{C}_6\text{D}_6$ ):  $\delta = -18$  ppm (s)

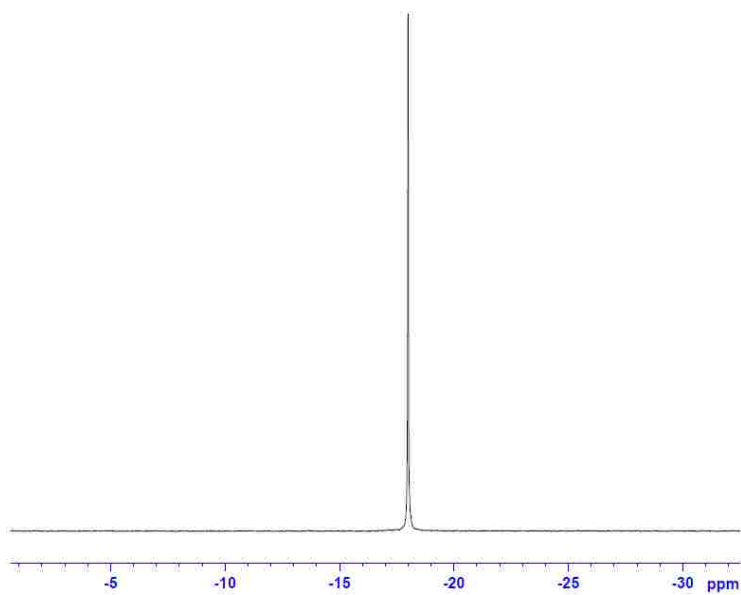


**Figure 4.12.**  $^{31}\text{P}\{^1\text{H}\}$  NMR of vinyl-diethylphosphine.

#### 4.13. Synthesis of *racemic* and *meso* et,ph-P4

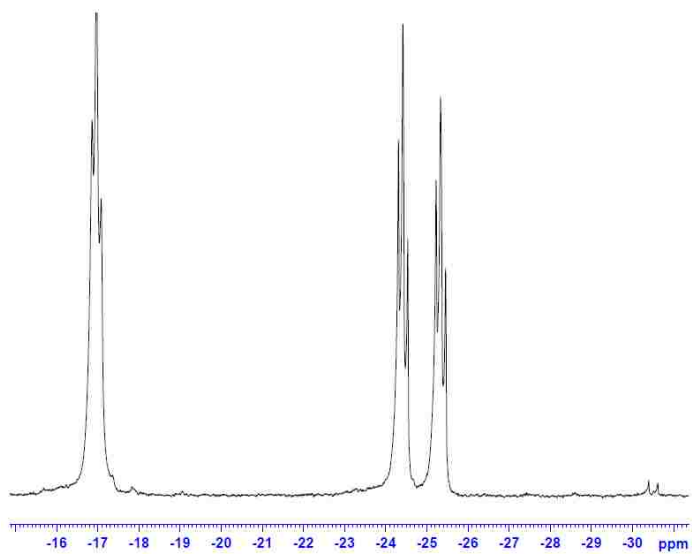


**Figure 4.13.**  $^{31}\text{P}\{^1\text{H}\}$  NMR of racemic and meso et,ph-P4.

Vinyldiethylphosphine (2.2 eq.) (13.0 g, 112 mmol) and bis(phenylphosphine)methane (1 eq.) (6.2 g, 27 mmol) are combined in a flask and irradiated with a UV light while stirring for at least 8 h. Excess vinyldiethylphosphine is removed in vacuo (90 °C) to result in a clear, slightly yellow, viscous liquid ( 12.5 g, 27 mmol).

Yield: 100%

$^{31}\text{P}\{^1\text{H}\}$  NMR ( $\text{C}_6\text{D}_6$ ):  $\delta = -16$  ppm (t) (arms),  $-24$  ppm (t) (racemic),  $-25$  ppm (t) (meso);  $[-30.3$  ppm (s) and  $-30.6$  (s) are impurities.

## VITA

Scott M. Boudreaux was born in Thibodaux, Louisiana, where he was raised by his parents, Herman and Janis Boudreaux, along with his brother, Joshua Boudreaux. He attended Nicholls State University in Thibodaux, where he obtained a Bachelor of Science in chemistry.

His search for knowledge continued by pursuing a master's degree in chemistry at Louisiana State University in Baton Rouge, Louisiana, in August 2008. His work under the guidance of Prof. George Stanley was to synthesize new ligands for use with a dirhodium hydroformylation catalyst. Although progress has been made, his work has not yet afforded these new ligands.